中国科技论文在线 http://www.paper.edu.cn

INSTITUTE OF PHYSICS PUBLISHING REPORTS ON PROGRESS IN PHYSICS

Rep. Prog. Phys. **68** (2005) 77–130 doi:10.1088/0034-4885/68/1/R02

The mass of the photon

Liang-Cheng Tu[1], Jun Luo[1,3] and George T Gillies[2]

[1] Department of Physics, Huazhong University of Science and Technology, Wuhan 430074, People's Republic of China
[2] School of Engineering and Applied Science, University of Virginia, Charlottesville, VA 22904, USA

E-mail: junluo@mail.hust.edu.cn and gtg@virginia.edu

Received 11 July 2004
Published 23 November 2004
Online at stacks.iop.org/RoPP/68/77

Abstract

Because classical Maxwellian electromagnetism has been one of the cornerstones of physics during the past century, experimental tests of its foundations are always of considerable interest. Within that context, one of the most important efforts of this type has historically been the search for a rest mass of the photon. The effects of a nonzero photon rest mass can be incorporated into electromagnetism straightforwardly through the Proca equations, which are the simplest relativistic generalization of Maxwell's equations. Using them, it is possible to consider some far-reaching implications of a massive photon, such as variation of the speed of light, deviations in the behaviour of static electromagnetic fields, longitudinal electromagnetic radiation and even questions of gravitational deflection. All of these have been studied carefully using a number of different approaches over the past several decades. This review attempts to assess the status of our current knowledge and understanding of the photon rest mass, with particular emphasis on a discussion of the various experimental methods that have been used to set upper limits on it. All such tests can be most easily categorized in terms of terrestrial and extra-terrestrial approaches, and the review classifies them as such. Up to now, there has been no conclusive evidence of a finite mass for the photon, with the results instead yielding ever more stringent upper bounds on the size of it, thus confirming the related aspects of Maxwellian electromagnetism with concomitant precision. Of course, failure to find a finite photon mass in any one experiment or class of experiments is not proof that it is identically zero and, even as the experimental limits move more closely towards the fundamental bounds of measurement uncertainty, new conceptual approaches to the task continue to appear. The intrinsic importance of the question and the lure of what might be revealed by attaining the next decimal place are as strong a draw on this question as they are in any other aspect of precise tests of physical laws.

[3] Author to whom any correspondence should be addressed.

0034-4885/05/010077+54$90.00 © 2005 IOP Publishing Ltd Printed in the UK

转载

中国科技论文在线 http://www.paper.edu.cn

Contents

	Page
1. Introduction	80
2. General theory of massive photon electromagnetism	81
3. Implications of a photon mass	83
3.1. The dispersion of light	83
3.2. The Yukawa potential in static fields	84
3.3. The longitudinal photon	84
3.4. Special relativity with nonzero photon mass	85
3.5. AB and AC effects with finite photon mass	85
3.6. Monopoles and the photon mass	87
3.7. The Casimir effect for massive photons	88
3.8. Photon mass and blackbody radiation	89
3.9. Other implications	90
4. Laboratory limits on the photon mass	90
4.1. General introduction	90
4.2. Measurement of the wavelength independence of the velocity of light	91
4.3. Null tests of Coulomb's inverse square law	94
4.3.1. Historical review of Coulomb's law	94
4.3.2. General method and technical background	98
4.3.3. Static experiments	99
4.3.4. Dynamic experiments	102
4.3.5. Other experiments	106
4.4. Tests of Ampère's law	106
4.5. Torsion balance methods	107
4.6. Other approaches	109
5. Extra-terrestrial limits on the photon mass	110
5.1. General introduction	110
5.2. Dispersion of starlight	110
5.3. Magnetostatic effects	112
5.3.1. Schrödinger external field	112
5.3.2. Altitude-dependence of massive photon geomagnetic fields	114
5.3.3. Eccentric dipole effects due to a massive photon	115
5.4. Magnetohydrodynamic effects	115
5.4.1. Dispersion of hydromagnetic waves	116
5.4.2. Dissipation of the interplanetary magnetic fields	117
5.4.3. Stability of current density in the ISM	119
5.4.4. Other methods	122
5.5. Gravitational deflection of massive photons	122
5.6. Present difficulties	122
6. Possible future improvements	124
6.1. Terrestrial experiments	124

中国科技论文在线 http://www.paper.edu.cn

6.2. Extra-terrestrial detection 125
6.3. Concluding remarks 125
Acknowledgments 126
References 126

中国科技论文在线 http://www.paper.edu.cn

1. Introduction

One of the major triumphs of nineteenth century physics was the formulation by Maxwell of a unified mathematical description of the classical electromagnetic field. A basic implication of Maxwell's electromagnetism is the constant speed, in vacuum, of all electromagnetic radiation. Experimental studies have indeed confirmed to a high degree of accuracy that all electromagnetic radiation travels at the speed of light, c, over a wide range of frequencies. In turn, this implies that the quantum of light, or photon, appears to be massless. However, it has energy $h\nu$, linear momentum $h\nu/c$, and a spin angular momentum with eigenvalues of $\pm h/2\pi (\equiv \pm\hbar)$, where h is the Planck constant and ν the frequency of the electromagnetic wave. The enormous successes of quantum electrodynamics (QED) have led to an almost total acceptance of this concept of the massless photon. However, despite this acceptance, a substantial experimental effort has been made to determine, either directly or indirectly, whether the photon mass is zero or nonzero. From a theoretical perspective, if the rest mass of the photon was found to be nonzero, classical electromagnetism and QED would remain untroubled in spite of the loss of gauge invariance. Moreover, a finite photon mass is perfectly compatible with the general principles of elementary particle physics, and an answer to the question of its size can be found only through experiments and/or observations.

It is almost certainly impossible to do any experiment that would firmly establish that the photon rest mass is exactly zero. The best one can hope to do is to place ever tighter limits on its size, since it might be so small that none of the present experimental strategies could detect it. According to the uncertainty principle, the ultimate upper limit on the photon rest mass, m_γ, can be estimated to be $m_\gamma \approx \hbar/(\Delta t)c^2$, which yields a magnitude of $\approx 10^{-66}$ g, using an age of the universe of about 10^{10} years. Although such an infinitesimal mass would be extremely difficult to detect, there are some far-reaching implications of a nonzero value for it. These include a wavelength dependence of the speed of light in free space, deviations from exactness in Coulomb's law and Ampère's law, the existence of longitudinal electromagnetic waves and the addition of a Yukawa component to the potential of magnetic dipole fields, and all of these have been studied seriously. All these consequences of such an effect open the door to useful approaches for laboratory experiments or astrophysical/cosmological observations aimed at determining the photon mass or, more precisely, setting an upper limit on it.

As the fundamental particle that mediates electromagnetic radiation, the photon conveys energy and momentum through space-time and propagates in vacuum at the constant velocity c, independent of the frame of reference, as per the second postulate of Einstein's theory of special relativity. A corollary of this is that a particle with finite mass can never attain the speed of light, c, or in other words, such a particle cannot exist in the frame of rest of a photon. The fact that light could not be brought to a stand-still made this point of view reasonable and it is theoretically difficult to find any kind of contradictory counter-example. Even so, experimental efforts to improve the limits on the rest mass of the photon have arisen to challenge contemporary accepted theories, and this has been happening since the time of Cavendish, if not earlier, and in any case well before the modern concept of the photon was introduced.

Questions central to the origin of and basis for the properties of elementary particles, such as the neutrino, photon, graviton, axion, etc, including their masses, charges, and even their existence, are some of the most challenging in physics. For the photon, the Particle Data Group finds the currently accepted upper limit on the rest mass to be $m_\gamma \leqslant 4 \times 10^{-49}$ g $\equiv 2 \times 10^{-16}$ eV (Hagiwara *et al* 2002). The improved value of $m_\gamma \leqslant 1 \times 10^{-49}$ g $\equiv 6 \times 10^{-17}$ eV was reported recently by Eidelman *et al* (2004). These numbers are quite impressively small; almost 22 orders of magnitude less than the mass of the electron. The possibility of a finite photon rest

中国科技论文在线 http://www.paper.edu.cn

mass remains one of the most important issues in physics, as it has a bearing on fundamental questions such as charge conservation and quantization, the possibility of charged black holes, the existence of magnetic monopoles and so on. It is our goal in this article to review the known experiments in this field and evaluate their impact on our state of knowledge regarding this question. In section 2, we introduce the theoretical foundation for massive photons, via a discussion of the Proca equations and the consequent distinctness of 'massive' electromagnetic fields compared with their purely Maxwellian equivalents. Using the Proca equations as a starting point, several possible observable effects associated with a nonzero rest mass of the photon are developed in section 3. In sections 4 and 5, we then review the known terrestrial and extra-terrestrial approaches to searching for such effects and assess the results found for upper limits on the photon rest mass. Section 6 closes the review with a discussion of the present limitations of and possible improvements to the experimental situation.

2. General theory of massive photon electromagnetism

Electromagnetic phenomena in vacuum are characterized by two three-dimensional vector fields, the electric and magnetic fields, $\boldsymbol{E}(\boldsymbol{x}, t)$ and $\boldsymbol{B}(\boldsymbol{x}, t)$, which are subject to Maxwell's equations and which can also be thought of as the classical limit (limit in large quantum numbers) of a quantum mechanical description in terms of photons. The photon mass is ordinarily assumed to be exactly zero in Maxwell's electromagnetic field theory, which is based on gauge invariance. If gauge invariance is abandoned, a mass term can be added to the Lagrangian density for the electromagnetic field in a unique way (Greiner and Reinhardt 1996):

$$L = -\frac{1}{4\mu_0} F_{\mu\nu} F^{\mu\nu} - j_\mu A^\mu + \frac{\mu_\gamma^2}{2\mu_0} A_\mu A^\mu, \tag{2.1}$$

where μ_γ^{-1} is a characteristic length associated with the photon rest mass, A_μ and j_μ are the four-dimensional vector potential $(\boldsymbol{A}, \mathrm{i}\phi/c)$ and four-dimensional vector current density $(\boldsymbol{J}, \mathrm{i}c\rho)$, with ϕ and $\boldsymbol{A}$ denoting the scalar and vector potentials, and ρ and $\boldsymbol{J}$ are the charge and current densities, respectively. μ_0 is the permeability constant of free space and $F_{\mu\nu}$ is the antisymmetric field strength tensor. It is connected to the vector potential through

$$F_{\mu\nu} = \frac{\partial A_\nu}{\partial x_\mu} - \frac{\partial A_\mu}{\partial x_\nu}. \tag{2.2}$$

The variation of Lagrangian density with respect to A_μ yields the Proca equation (Proca 1930a,b,c, 1931, 1936a,b,c,d, 1937, 1938, de Broglie 1940):

$$\frac{\partial F_{\mu\nu}}{\partial x_\nu} + \mu_\gamma^2 A_\mu = \mu_0 J_\mu. \tag{2.3}$$

Substituting equation (2.2) into (2.3), we obtain the wave equation of the Proca vector field A_μ:

$$(\Box - \mu_\gamma^2) A_\mu = -\mu_0 J_\mu, \tag{2.4}$$

where the d'Alembertian symbol $\Box$ is shorthand for $\nabla^2 - \partial^2/\partial(ct)^2$. In free space, equation (2.4) reduces to

$$(\Box - \mu_\gamma^2) A_\mu = 0, \tag{2.5}$$

which is essentially the Klein–Gordon equation for the photon. The parameter μ_γ could be interpreted as the photon rest mass m_γ, with

$$m_\gamma = \frac{\mu_\gamma \hbar}{c}. \tag{2.6}$$

中国科技论文在线 http://www.paper.edu.cn

With this interpretation, the characteristic scaling length μ_γ^{-1} becomes the reduced Compton wavelength of the photon, which is the effective range of the electromagnetic interaction. An additional point is that static electric and magnetic fields would exhibit exponential damping governed by the term $\exp(-\mu_\gamma^{-1} r)$ if the photon is massive instead of massless.

Therefore, a finite photon mass is accommodated in a unique way by changing the inhomogeneous Maxwell's equations to the Proca equations. In the presence of sources ρ and $\boldsymbol{J}$, the three-dimensional versions of the Proca equations can be written in SI units as

$$\nabla \cdot \boldsymbol{E} = \frac{\rho}{\varepsilon_0} - \mu_\gamma^2 \phi, \tag{2.7}$$

$$\nabla \times \boldsymbol{E} = -\frac{\partial \boldsymbol{B}}{\partial t}, \tag{2.8}$$

$$\nabla \cdot \boldsymbol{B} = 0, \tag{2.9}$$

$$\nabla \times \boldsymbol{B} = \mu_0 \boldsymbol{J} + \mu_0 \varepsilon_0 \frac{\partial \boldsymbol{E}}{\partial t} - \mu_\gamma^2 \boldsymbol{A}, \tag{2.10}$$

together with

$$\boldsymbol{B} = \nabla \times \boldsymbol{A}, \tag{2.11}$$

$$\boldsymbol{E} = -\nabla \phi - \frac{\partial \boldsymbol{A}}{\partial t} \tag{2.12}$$

and the Lorentz condition

$$\nabla \cdot \boldsymbol{A} + \frac{1}{c^2} \frac{\partial \phi}{\partial t} = 0, \tag{2.13}$$

where ε_0 and μ_0 are the permittivity and permeability of free space, respectively. The Proca equations provide a complete and self-consistent description of electromagnetic phenomena. The equation for conservation of charge is obtained from equations (2.7) and (2.10) and the Lorentz condition (2.13), so that

$$\nabla \cdot \boldsymbol{J} + \frac{\partial \rho}{\partial t} = 0. \tag{2.14}$$

Obviously, in massive photon electromagnetism, the Lorentz condition is identical to the law of charge conservation, or in other words, the Lorentz condition is a necessary result of charge conversation. Similarly, from equations (2.9), (2.10), (2.12) and (2.13), the equation for conservation of energy can be written as

$$\nabla \cdot \boldsymbol{S} + \frac{\partial w}{\partial t} = -\boldsymbol{J} \cdot \boldsymbol{E}, \tag{2.15}$$

where the Poynting vector, $\boldsymbol{S}$, represents the energy flow density and w is the energy density of the electromagnetic field (de Broglie 1940, Bass and Schrödinger 1955, Burman 1972a):

$$\boldsymbol{S} = \frac{1}{\mu_0} (\boldsymbol{E} \times \boldsymbol{B} + \mu_\gamma^2 \phi \boldsymbol{A}) \tag{2.16}$$

and

$$w = \frac{1}{2} \left(\varepsilon_0 \boldsymbol{E}^2 + \frac{1}{\mu_0} \boldsymbol{B}^2 + \varepsilon_0 \mu_\gamma^2 \phi^2 + \frac{1}{\mu_0} \mu_\gamma^2 \boldsymbol{A}^2 \right). \tag{2.17}$$

In a Proca field, obviously, the potentials themselves have physical significance; it does not arise just through their derivatives. The scalar potential ϕ and the vector potential $\boldsymbol{A}$ described by the Proca equations are observable since the potentials acquire energy density $\varepsilon_0 \mu_\gamma^2 \phi^2/2$ and $\mu_\gamma^2 \boldsymbol{A}^2/2\mu_0$, respectively. Phase invariance ($U(1)$ invariance) is lost in Proca theory, but the

中国科技论文在线 http://www.paper.edu.cn

Lorentz gauge is automatically held, and this is indispensable to charge conservation, i.e. the Lorentz condition becomes a condition of consistency for the Proca field. As a consequence, the field equation takes the form of equation (2.4). However, if $m_\gamma = 0$, the Proca equations would reduce smoothly to Maxwell's equations.

The theoretical problem of describing the photon is profound and difficult, and the arguments presented can often be speculative and controversial. There is a huge literature on this topic and the articles in it vary widely in their scope of investigation. A number of the more well-known works in this area include (Feynman 1949, Coester 1951, Feldman and Matthews 1963, Strocchi 1967, Chakravorty 1985, Masood 1991, Mendonça *et al* 2000). Although the theoretical problem is an area of great interest, it is not our objective here to dwell on it, but rather to touch only on those fundamental principles that can help shed light on the experimental consequences of a nonzero photon rest mass.

3. Implications of a photon mass

3.1. The dispersion of light

The most direct consequence of a finite photon mass is a frequency dependence in the velocity of electromagnetic waves propagating in free space. From the Proca equations, the electric and magnetic fields in free space are given by

$$A_\nu \sim \exp[\mathrm{i}(\boldsymbol{k}\cdot\boldsymbol{r} - \omega t)], \tag{3.1}$$

where the wave vector $\boldsymbol{k}$, the angular frequency ω and the rest mass μ_γ (note that here and in what follows, the rest mass of the photon μ_γ has units of reciprocal length (wave numbers), which is related to the mass m_γ in grams by equation (2.6), i.e. $1\,\mathrm{cm}^{-1} \equiv 3.5 \times 10^{-38}\,\mathrm{g} \equiv 2.0 \times 10^{-5}\,\mathrm{eV}$) satisfy the Klein–Gordon equation,

$$k^2c^2 = \omega^2 - \mu_\gamma^2 c^2. \tag{3.2}$$

The phase velocity and the group velocity (the velocity of energy flow) of a free massive wave would then take the form

$$u = \frac{\omega}{k} = c\left(1 - \frac{\mu_\gamma^2 c^2}{\omega^2}\right)^{-1/2} \approx c\left(1 + \frac{\mu_\gamma^2 c^2}{2\omega^2}\right), \tag{3.3}$$

$$v_\mathrm{g} = \frac{\mathrm{d}\omega}{\mathrm{d}k} = c\left(1 - \frac{\mu_\gamma^2 c^2}{\omega^2}\right)^{1/2} \approx c\left(1 - \frac{\mu_\gamma^2 c^2}{2\omega^2}\right), \tag{3.4}$$

where $k = |\boldsymbol{k}| = 2\pi\lambda^{-1}$ with λ being the wavelength. Because of the nonzero photon mass, the dispersion produces a frequency dependence, and the group velocity will differ from the phase velocity. In the Proca equations, c becomes the limiting velocity as the frequency approaches infinity.

For two wave packets with different propagating frequencies (denoted by ω_1 and ω_2, and assuming $\omega_1 > \omega_2 \gg \mu_\gamma c$), the velocity differential between them is given by

$$\frac{\Delta v}{c} \equiv \frac{v_{\mathrm{g}1} - v_{\mathrm{g}2}}{c} = \frac{\mu_\gamma^2 c^2}{2}\left(\frac{1}{\omega_2^2} - \frac{1}{\omega_1^2}\right) + \mathrm{O}\left[\left(\frac{\mu_\gamma^2 c^2}{\omega_1^2}\right)^4\right] = \frac{\mu_\gamma^2}{8\pi^2}(\lambda_2^2 - \lambda_1^2) + \mathrm{O}\left[(\mu_\gamma\lambda_1)^4\right]. \tag{3.5}$$

中国科技论文在线 http://www.paper.edu.cn

If the two waves move through the same distance L, the time interval between their arrivals is expressed as

$$\Delta t \equiv \frac{L}{v_{g1}} - \frac{L}{v_{g2}} \approx \frac{L}{8\pi^2 c}(\lambda_2^2 - \lambda_1^2)\mu_\gamma^2, \tag{3.6}$$

in which the terms of order higher than $(\mu_\gamma \lambda_1)^4$ are neglected. Equations (3.4)–(3.6) are the starting points for detecting a dispersion effect due to the photon rest mass in both the terrestrial and extra-terrestrial approaches.

3.2. The Yukawa potential in static fields

The next effect we discuss regarding massive photons arises in static fields. For a static electric field (the case of a static magnetic field will be discussed in section 5), $\partial/\partial t = 0$ and the wave equation reduces to

$$(\nabla^2 - \mu_\gamma^2)\phi = -\frac{\rho}{\varepsilon_0}. \tag{3.7}$$

For a point charge $\rho(r) = Q\delta(r)$, and equation (5.25) yields a Yukawa or Debye type of potential,

$$\phi(r) = \frac{1}{4\pi\varepsilon_0}\frac{Q}{r}\exp(-\mu_\gamma r) \tag{3.8}$$

and the electric field becomes

$$E(r) = \frac{Q}{4\pi\varepsilon_0}\left(\frac{1}{r^2} + \frac{\mu_\gamma}{r}\right)\exp(-\mu_\gamma r). \tag{3.9}$$

Inspection of equations (3.8) and (3.9) shows that if $r \ll \mu_\gamma^{-1}$, the inverse square law is indeed a good approximation, but if $r \gg \mu_\gamma^{-1}$, then the law departs drastically from the predictions of Maxwell's equations. (Analogously, in a plasma, the static scalar potential does have a Debye form,

$$\phi(r) = \frac{1}{4\pi\varepsilon_0}\frac{Q}{r}\exp(-\mu_D r), \tag{3.10}$$

where $\mu_D = \sqrt{n\,e^2/\varepsilon_0 T}$ is the inverse Debye shielding distance, n is the plasma density and T (in joules) is the plasma temperature. Likewise, in a superconductor, a static magnetic field obeys

$$(\nabla^2 - \mu_L^2)\boldsymbol{B} = 0, \tag{3.11}$$

where $\mu_L = \omega_p/c$ is the London skin depth, with $\omega_p = \sqrt{ne^2/\varepsilon_0 m_e}$ denoting the electron plasma frequency.) So the static fields would be characteristic of exponential decay with a range μ_γ^{-1}. The exponential deviation from Coulomb's law and its magnetic analogue in Ampère's law provide many sensitive approaches to test for a photon rest mass in laboratory experiments, and these will be discussed in detail in section 4.

3.3. The longitudinal photon

Maxwell's equations imply that a photon can be polarized in either of two directions, both of which are orthogonal to the photon's direction of motion. A nonzero rest mass of the photon as described by the Proca equations would result in a third state of polarization, in which the vector of the electric field points along the line of motion and the particle is called a 'longitudinal photon' (Greiner and Reinhardt 1996). Decomposition of $\boldsymbol{E} = \boldsymbol{E^T} + \boldsymbol{E^L}$ with

中国科技论文在线 http://www.paper.edu.cn

$\nabla \cdot \boldsymbol{E}^{\boldsymbol{T}} = 0$ and $\boldsymbol{E}^{\boldsymbol{L}} = \nabla E^{L}$, and a similar decomposition of $\boldsymbol{A}$, shows that the additional mass term in equation (2.16) describes pure longitudinal radiation while the term $(\boldsymbol{E} \times \boldsymbol{B})$ describes pure transverse radiation, in which $(\boldsymbol{E}^{\boldsymbol{L}} \times \boldsymbol{B})$ is parallel to the surface of a large sphere around the source (Nieuwenhuizen 1973). However, if the photon has a mass, it must be exceedingly small, since the effect of longitudinal photons has been too small to be detected up to the present (Goldhaber and Nieto 1971b, Burman 1972b,c, 1973).

3.4. Special relativity with nonzero photon mass

It is well-known that the electrodynamic constant c in Maxwell's electromagnetic field represents the velocity of electromagnetic waves propagating in vacuum, and special relativity was developed partly as a consequence of the constancy of the speed of light. However, one of the predictions of massive photon electromagnetic theory is that there will be dispersion of the velocity of a massive photon in vacuum. The plane wave solution of the Proca equations without current is $A^{\nu} \sim \exp(\mathrm{i}k^{\mu}x_{\mu})$, where the wave vector $k^{\mu} = (\omega, \boldsymbol{k})$ satisfies the relationship in equation (3.2). It is shown in equation (3.4) that $v_{\mathrm{g}} = 0$ for $\omega = \mu_{\gamma}c$, namely the massive wave does not propagate. When $\omega < \mu_{\gamma}c$, k becomes an imaginary quantity and the amplitude of a free massive wave would, therefore, be attenuated exponentially. Only when $\omega > \mu_{\gamma}c$, can the waves propagate in vacuum unattenuated. In the limit $\omega \to \infty$, the group velocity will approach the constant c, which is consistent with Einstein's assumption that there is a unique limiting velocity c for all phenomena. Therefore, a new postulate must be introduced in order to restore the features of special relativity theory for photons of nonzero mass. The postulate is as follows (Goldhaber and Nieto 1971b): given any two inertial frames, the first moving at velocity $\boldsymbol{v}$ with respect to the second, there exists a frequency ω_0, depending on $|\boldsymbol{v}|$ and the desired accuracy ε, such that any light wave of frequency greater than ω_0 will have a speed between c and $c - \varepsilon$ in both frames.

A nonzero photon mass implies that the speed of light is not a unique constant but is a function of frequency. In fact, the assumption of the constancy of the speed of light is not necessary for the validity of special relativity, i.e. special relativity can instead be based on the existence of a unique limiting speed c to which speeds of all bodies tend when their energy becomes much larger than their mass (Kobzarev and Okun 1968, Goldhaber and Nieto 1971b). Then, the velocity that enters in the Lorentz transformation would simply be this limiting speed, not the speed of light.

3.5. AB and AC effects with finite photon mass

The well-known topological interference effect of Aharonov and Bohm (AB effect) concerns a phase shift for electrons diffracting around a tube of magnetic flux (Aharonov and Bohm 1959), and it arises from the presence of a vector potential $\boldsymbol{A}$ in the Lagrangian of a particle with mass m and velocity $\boldsymbol{v}$,

$$L = \frac{mv^2}{2} + e\boldsymbol{A} \cdot \boldsymbol{v}. \tag{3.12}$$

When an electron beam is split and then recombined, there will be a phase shift $\exp(\mathrm{i}\Phi_{\mathrm{AB}})$ from the interference effect (figure 1). The flux

$$\Phi_{\mathrm{AB}} = \frac{e}{\hbar} \oint \boldsymbol{A} \cdot \boldsymbol{v}\, \mathrm{d}t = \frac{e}{\hbar} \int \boldsymbol{B} \cdot \mathrm{d}\boldsymbol{S} \tag{3.13}$$

is through any surface bounded by the closed curve defined by the two paths, and it has been observed and measured in a series of experiments of Tonomura *et al* (1986).

中国科技论文在线 http://www.paper.edu.cn

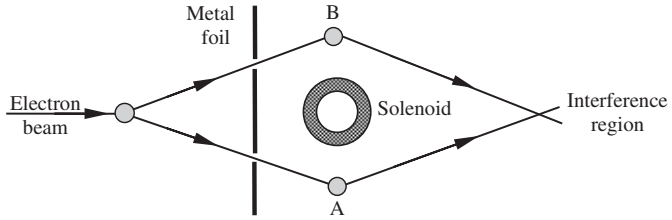


Figure 1. Schematic diagram of an experiment to demonstrate electron interference due to the Aharonov–Bohm effect. The coherent beam of electrons is split into two parts, each passing through an aperture in the metal foil, and then going on the opposite sides of the solenoid, which is shielded from the electron beams. The beams are steered by suitable devices A and B and then brought together in the interference region. The vector potential of the solenoid will produce a shift in the relative phase of the two electron beams.

For massive photon (finite-range) electrodynamics, the Proca Lagrangian is of particular interest and the resultant phase shift for an electron beam diffracted around either side of an infinitely long solenoid was calculated by Boulware and Deser (1989). Although there is an extremely small magnetic flux leakage outside the solenoid because of the finite length of the apparatus, it can be adjusted in principle so that only the flux inside the solenoid contributes to the phase shift. The phase shift for this case is shown to reduce smoothly to that of the standard AB effect in the limit of vanishing photon mass. An additional observable effect is predicted from

$$\left(\frac{\mu_\gamma R}{2}\right)^2 \geqslant \frac{\Delta\Phi}{\Phi_{\mathrm{AB}}} \cdot D, \tag{3.14}$$

where D depends upon the details of the experimental configuration but is of order 1, R is the distance from the solenoid to the observational location, and $\Delta\Phi$ is the correction due to the massive photon. The authors used this to find a limit on the photon mass of $m_\gamma \leqslant 4 \times 10^{-45}$ g (corresponding to a reduced photon Compton wavelength of 10^2 km). To obtain a more stringent limit on the photon mass, however, the geometry and field strengths that would be needed do not make this approach competitive with those of other experiments (Tonomura *et al* 1986, Boulware and Deser 1989).

An extension of the AB effect was presented by Aharonov and Casher (AC effect) (1984). They predicted that a neutral particle possessing a magnetic dipole moment should experience an analogous phase shift when diffracted around a line of electric charge. The AC effect is an electrodynamic and quantum-mechanical analogue of the AB effect. Consider a magnetic dipole of mass m and moment $\boldsymbol{\mu}$ diffracted around an infinitely long line of charge with density λ and let $\boldsymbol{v}$ be the dipole's velocity; the particle's Lagrangian will be

$$L = \tfrac{1}{2}mv^2 - \boldsymbol{v} \cdot (\boldsymbol{E} \times \boldsymbol{\mu}). \tag{3.15}$$

The relative phase of the split beam at the recombination point is $\exp(\mathrm{i}\Phi_{\mathrm{AC}})$ with

$$\Phi_{\mathrm{AC}} = \frac{\boldsymbol{\mu}}{\hbar} \cdot \oint \boldsymbol{E} \times \boldsymbol{v}\,\mathrm{d}t = \frac{\boldsymbol{\mu}}{\hbar} \cdot \oint \boldsymbol{E} \times\, \mathrm{d}\boldsymbol{r}, \tag{3.16}$$

as was observed in the neutron interferometry experiment of Cimmino *et al* (1989).

The AC effect in massive photon electrodynamics was demonstrated by Fuchs (1990). Consider the case where a magnetic dipole of moment $\boldsymbol{\mu}$ is aligned along the line of electric charge, which means the acceleration of the magnetic dipole vanishes and the AC phase shift

中国科技论文在线 http://www.paper.edu.cn

for the massive photon case then becomes

$$\Phi_{\mathrm{AC}} = \frac{\mu}{\hbar}\int (\nabla \cdot \boldsymbol{E})\,\mathrm{d}S = \frac{4\pi\mu\lambda}{\hbar} - \frac{\mu_\gamma^2\mu}{\hbar}\int \phi\,\mathrm{d}S, \tag{3.17}$$

where the Proca version of Gauss's law is used and the integral is taken over the area enclosing the two paths. Noting that the potential for a point particle whose field is governed by the Proca equations is simply the Yukawa potential, the line charge potential is found to be

$$\phi(r) = 2\lambda K_0(\mu_\gamma r), \tag{3.18}$$

where $K_0(x)$ is a modified Bessel function of the second kind. After integrating, the relative phase of the split beam at the recombination point R is

$$\Phi_{\mathrm{AC}}(R) = \frac{4\pi\mu\lambda}{\hbar}\mu_\gamma R K_1(\mu_\gamma R). \tag{3.19}$$

Note that since $K_1(x)$ approaches x^{-1} as x vanishes, $\Phi_{\mathrm{AC}}(R)$ approaches $4\pi\mu\lambda/\hbar$ as μ_γ vanishes, which means this effect smoothly reduces to the standard effect for zero μ_γ (Aharonov and Casher 1984). In the limit that R approaches infinity, $\Phi_{\mathrm{AC}}(R)$ vanishes. This is as expected since the photon mass causes the electric field to be of finite range. Equation (3.19) can serve as the basis for a photon mass with a 'table-top' apparatus. However, the neutron interferometry experiment of Cimmino *et al* (1989) revealed that only photons with a Compton wavelength of 10 m or less can be detected by these means. So given present-day technology, this is not a practical approach for bounding the photon mass.

In classical electrodynamics, both the AB and AC effects are nonlocal effects for nongauge fields, such as for those associated with a finite photon mass. In the AB effect, the flux must be endless but could be curved arbitrarily, even into a finite toroid, but in the AC effect, the line charge must be straight and parallel to the magnetic moment (Goldhaber 1989). Given present-day technologies, neither the AB nor AC effects would provide a practical means for bounding the mass of the photon more stringently.

3.6. Monopoles and the photon mass

An interesting speculation centres on the combination of a finite photon mass, μ_γ and the existence of magnetic monopoles. Gauge invariance is lost in massive photon electrodynamics. Therefore, one cannot apply it (Dirac 1931, 1948) to derive the well-known Dirac quantization condition that $eg/\hbar c$ is a half-integer with e and g being the elementary electric and magnetic charges, respectively. In fact, Dirac's approach would not allow any gauge invariant theory to include a particle that is the source of a r^{-2} magnetic field with additional 'Yukawa' falloff (Goldhaber and Nieto 1971b). Ignatiev and Joshi (1996) further proved that the Dirac quantization condition cannot be derived in massive photon electrodynamics because gauge invariance disappears, thus pointing to the conclusion that the Dirac monopole and the finite mass photon cannot coexist within the same theory (Ignatiev and Joshi 1996, Singleton 1996).

In classical theory, Maxwell's equations can be generalized to include magnetic charge and a finite photon mass. They, then, become

$$\nabla \cdot \boldsymbol{E} = \frac{\rho}{\varepsilon_0} - \mu_\gamma^2\phi, \tag{3.20}$$

$$\nabla \times \boldsymbol{E} = -\frac{\partial \boldsymbol{B}}{\partial t} - \varepsilon_0 \boldsymbol{J}_{\mathrm{g}}, \tag{3.21}$$

$$\nabla \cdot \boldsymbol{B} = \mu_0\rho_{\mathrm{g}}, \tag{3.22}$$

$$\nabla \times \boldsymbol{B} = \mu_0\boldsymbol{J} + \mu_0\varepsilon_0\frac{\partial \boldsymbol{E}}{\partial t} - \mu_\gamma^2\boldsymbol{A} \tag{3.23}$$

together with the relations in equations (2.11)–(2.13).

中国科技论文在线 http://www.paper.edu.cn

It is clear from these equations that the photon mass terms $\mu_\gamma^2\phi$ and $\mu_\gamma^2\boldsymbol{A}$ on the right-hand side violate the symmetry between the electric and magnetic charges. The electric equation (3.20) has a solution of the familiar Yukawa-potential form, while the magnetic equation (3.22) does not cover the photon mass at all. Therefore, the system of 'Maxwell + photon mass + magnetic charge' equations is not consistent, as can be verified by investigating a static monopole-like solution of that system (Ignatiev and Joshi 1996).

3.7. The Casimir effect for massive photons

It is well-known that the Casimir force is an attractive force between two neutral conducting plates (Casimir 1948, Casimir and Polder 1948). This interaction arises from zero-point fluctuations, which are a rare macroscopic manifestation of the boundary dependence of the quantum vacuum. The attractive force F (per unit area) between two perfectly conducting slabs separated by a distance $2L$ is (see the monographs of Mostepanenko and Trunov (1997) and Milton (2001) and the reviews by Kardar and Golestanian (1999) and Bordag *et al* (2001))

$$F = -\frac{\pi^2}{240}\frac{\hbar c}{(2L)^4} = -\frac{\partial U}{\partial(2L)}, \tag{3.24}$$

$$U = -\frac{\pi^2}{720}\frac{\hbar c}{(2L)^3}. \tag{3.25}$$

Massive photon electrodynamics contains a new characteristic length scale, the Compton wave length, which will lead to new physical effects over the length scale, including the Casimir effect. To calculate the Casimir force with finite photon mass, one must obtain the dependence of the total zero point energy of the system on the plate separation $2L$, and then sum over all the frequencies of the Proca solutions. A complete analysis of the Proca normal-mode structure for parallel-plane geometry shows that the Casimir force comes from two contributions: one is the Maxwellian modes and the other is the continuum modes (Barton and Dombey 1984, 1985, Davies and Toms 1985).

The Maxwellian modes represent two independent solutions of the Proca equations, which correspond to the two independent and transverse solutions of Maxwell's theory. The calculation of the zero point energy from the Maxwellian modes is straightforward and can be performed on the basis of dimensional regularization (Ambjorn and Wolfram 1983) and the appropriate dispersion relation including the photon mass (Barton and Dombey 1984, 1985), which is

$$U_1(L) = -\frac{\pi^2}{3(2L)^3}\int_\mu^\infty \frac{\mathrm{d}\rho(\rho^2-\mu^2)^{3/2}}{\mathrm{e}^{2\pi\rho}-1}, \tag{3.26}$$

where $\mu = 2L\mu_\gamma/\pi$. Approximating this expression for the case of small μ yields

$$U_1(L) = \frac{\pi^2}{(2L)^3}\left[-\frac{1}{720}+\frac{1}{48}\mu^2-\frac{1}{12}\mu^3-\frac{1}{16}\mu^4\ln\mu+\cdots\right]. \tag{3.27}$$

The first term gives the normal Casimir attractive force, and the lowest finite-mass correction tends to reduce the effect.

The continuum modes represent a new class of solution with a continuous spectrum for the Proca equations, which does not exist for Maxwell's equations. Since the continuum (longitudinal) modes can penetrate the conductors, one should consider the two conducting plates to be of finite thickness N. The general expression for zero point energy from the continuum modes is (Barton and Dombey 1984)

$$U_2(L) = \frac{\pi^2}{(2L)^3}f(\mu_\gamma L, \mu_\gamma N), \tag{3.28}$$

中国科技论文在线 http://www.paper.edu.cn

where in the most favourable configuration, $L \ll N$, one finds (for the realistic case $\mu_\gamma L, \mu_\gamma N \ll 1$)

$$f \sim \frac{1}{2\pi^2}(\mu_\gamma L)^4 \ln \frac{N}{4L}. \tag{3.29}$$

This contribution to the Casimir force can be negligible, compared with the leading finite-mass correction to the contribution from the transverse modes. Based on the present experimental precision (the recent experimental work is discussed in Chen *et al* (2004)), no prominent reduction in the bounds on the photon mass is achieved.

3.8. Photon mass and blackbody radiation

If the photon had a nonzero rest mass, one might initially expect a photon gas to have two transverse degrees and one longitudinal degree of freedom. This would alter Planck's radiation law by a factor of 3/2, in contradiction with experience. Although dynamical symmetry breaking of the standard model is ruled out, much interest has been shown in possible spontaneous symmetry breaking (Dombey 1980, Primack and Sher 1980, Abbott and Gavela 1982, Georgi *et al* 1983, Nussinov 1987, Mohapatra 1987, Suzuki 1988).

Dombey (1980) argued that spontaneous $U(1)$ symmetry breaking would imply that a gauge particle, the photon, would become massive at a low enough temperature, or more exactly, a photon gas in equilibrium with a heat bath would undergo a phase transition at $T = T_c$ so that at temperatures below T_c, each photon in the gas would have a nonzero mass $\mu_\gamma(T)$. Above this phase-transition temperature, the photon is strictly massless. Primack and Sher (1980) claimed that present limits on the photon mass show only that m_γ is negligible for $T > 2.7\,\mathrm{K} \sim 10^{-4}\,\mathrm{eV}$. Meanwhile, they argued that they have not found a proper explanation for this electromagnetic gauge-symmetry breaking and, therefore, cannot estimate T_c or m_γ. However, Abbott and Gavela (1982) pointed out that the scenario proposed by Primack and Sher is impossible. Their thought was that a virtual photon propagating through thermal radiation at normal laboratory temperatures is completely unaffected simply because there is no existing mechanism to interact with the thermal photons in any appreciable way. Therefore, it is completely valid and applies to experiments regardless of whether they are carried out at room temperature or at absolute zero.

Nevertheless, according to an argument by Bass and Schrödinger (1955), the interaction of longitudinal photons with matter would be so feeble as to make them irrelevant for the equilibration of thermal radiation in a perfectly reflecting cavity: its walls would be essentially transparent to them. Stueckelberg (1941, 1957) first investigated QED with a massive photon and concluded that amplitudes describing longitudinal modes tended continuously to zero as $\mu_\gamma \to 0$, provided that electromagnetic current is conserved.

In a cavity with volume V, the partition function Z is given by $\ln Z = \lambda \ln \sum_n \exp(-\beta\varepsilon_n)$ (Hernandez 1985), where λ is the number of photon polarizations and $\varepsilon_n = h\upsilon = (((h^2c^2)/(4V^{2/3}))n^2 + m_\gamma^2 c^4)^{1/2}$, which leads to the spectral distribution

$$\rho(\upsilon, m_\gamma, T) = \rho_P(\upsilon, T)\sqrt{1 - \left(\frac{m_\gamma c^2}{h\upsilon}\right)^2}, \tag{3.30}$$

where $\rho_P(\upsilon, T) = ((2\pi)/(c^2))((h\upsilon^3)/(\mathrm{e}^{h\upsilon/kT} - 1))$ is the Planck spectrum. At very low temperatures $kT \ll m_\gamma c^2$, the radiance $R = \int \rho \, \mathrm{d}\upsilon$ will approach zero exponentially, and at high temperatures $kT \gg m_\gamma c^2$ (Hernandez 1985),

$$R = \sigma_{SB} T^4 \left(1 - \frac{5}{4\pi^2}\left(\frac{m_\gamma c^2}{kT}\right)^2\right), \tag{3.31}$$

中国科技论文在线 http://www.paper.edu.cn

where $\sigma_{SB} = 2\pi^5 k^4/(15h^3c^2)$ is the theoretical value of the Stefan–Boltzmann constant. Unfortunately, the relatively large uncertainties in knowledge of σ_{SB} makes this an unpractical means for bounding the photon mass. (The fractional error of $\Delta\sigma/\sigma \sim 10^{-3}$ at $T = 10^3$ K implies $m_\gamma < 10^{-35}$ g.) For the case of the cosmic blackbody radiation (CBR), assuming that the CBR flux corresponds to a slight distortion of a $T = 3$ K Planck distribution, an approximate error of 10% produced a bound of order 10^{-37} g for the photon rest mass.

Following the hypothesis of Georgi *et al* (1983), de Bernardis *et al* (1984) have investigated the effects of photon mass on the spectral behaviour of the cosmic background dipole anisotropy, and found a distortion increasing with wavelength to such an extent that the direction of the dipole anisotropy can be reversed. The best fit of the available but not totally reliable experimental data gave a value for the photon mass of $(2.9 \pm 0.1) \times 10^{-51}$ g with a confidence level of 68%. However, as they claimed, the evidence for nonzero photon mass is based essentially on the long wavelength dipole anisotropy data. Thus, a larger collection of high spectral resolution data would be important in order to claim the existence of photon mass, as this quantity is extremely sensitive to photon oscillation in the dipole anisotropy.

3.9. Other implications

Besides those special cases discussed above, the massive photon effect should manifest itself, in principle, in almost all electromagnetic phenomena that obey Maxwell's equations. But not all such phenomena are either observable or would be practical to implement. So the experimental efforts to tighten the limits on the photon rest mass are greatly restrained. In some new theories, useful approaches may be found in the near future to set more stringent bounds on the photon rest mass. These might include, for instance, string theory or M-theory (Kostelecký and Samuel 1991, Arkani-Hamed *et al* 1998), extended electromagnetic theory (Davies and Toms 1985, Lehnert and Roy 1998, Lehnert 2000), B(3) field theory (Evans and Vigier 1994, Evans and Crowell 2001), new weak force predictions, and others (Bartlett and Lögl 1988, Cameron *et al* 1993, Krause *et al* 1994, Kloor *et al* 1994, Jackson and Okun 2001, Prokopec *et al* 2002, Kohler 2002). Although many of these authors discuss very interesting possibilities, further discussion of them is beyond the scope of this review, which will focus in what follows on the experimental and observational findings.

4. Laboratory limits on the photon mass

4.1. General introduction

Photons, just like any other observed particle, possess a real physical identity and are not just a conceptualization of the physicist's mind. Once the photon is provided with a finite mass, three immediate consequences may be deduced from the Proca equations: (1) there will be a frequency dependence in the velocity of light propagating in free space, (2) a third state of polarization, viz, the 'longitudinal photon' will exist and (3) there will be some modifications in the characteristics of the classical static fields. Critical scientific minds since the time of Cavendish and before have repeatedly come to the conclusion that the photon may have mass. The question is a persistent one and has spurred several reviews of the topic over the past 30 years (Goldhaber and Nieto 1971b, Chibisov 1976, Byrne 1977, Dolgov and Zeldovich 1981, Vigier 1990, 1992, 1997, Gray 1997, Zhang 1998). In this section, we will discuss the history of the various experimental searches for the photon mass that have been carried out in the terrestrial laboratory or on the surface of the earth.

中国科技论文在线 http://www.paper.edu.cn

4.2. Measurement of the wavelength independence of the velocity of light

Over the past 300 years, and especially during the last century, the speed of light was measured frequently and repeatedly using several different laboratory approaches and astronomical methods. The continual advancement of measurement technology led to considerable improvements in the precision and accuracy of those measurements. There is an extensive literature on the subject and it has been covered in a long series of reviews which, in temporal order, are by Birge (1941a,b), Dorsey (1944), Mulligan (1952), Mulligan and McDonald (1957), Taylor *et al* (1969), Froome and Essen (1969), Mulligan (1976), Wilkie (1983) and more recently by Norman and Setterfield (1987), and partly by Flowers and Petley (2001). Current scientific opinion is that the speed of light is a fixed and immutable constant of nature, and represents the fastest possible speed in the physical universe. In October 1983 the speed of light, c, was declared to be a universal constant of nature whose value was known exactly and defined as 299 792 458 m s^{-1} and was then subsequently incorporated into the definition of the metre by the General Conference on Weights and Measures, in Paris (Wilkie 1983). To be precise, what is routinely referred to as the 'speed of light' is really the speed of light in vacuum (the absence of matter). However, the speed of light of course depends on the material or medium through which it is propagating. Thus, for example, light moves slower in glass than in air and in both cases the speed is less than in vacuum. However, the density of matter between the stars is sufficiently low that the actual speed of light through most of interstellar space is essentially the speed that it would have through the vacuum.

The second postulate of special relativity is that the speed of light has the same value in all inertial frames, although this had not yet been tested when it was proposed by Einstein. From this and the postulate that the form of physical laws remains the same in all inertial systems, Einstein then derived the Lorentz transformations, which Lorentz himself had already used to demonstrate form invariance of Maxwell's equations. The investigations of the invariance of the speed of light are usually grouped into three different categories (Robertson 1949, Mansouri and Sexl 1977): measurements of the isotropy of space (Michelson–Morley experiments), independence of the speed of light from the velocity of the source (Kennedy–Thorndike experiments), and time dilation experiments (typically based on Doppler spectroscopy). Some high precision recent examples of all three types of experiments show how the various techniques have been improved over the years (Young 1999, Braxmaier *et al* 2002, Lipa *et al* 2003, Wolf *et al* 2003, Müller *et al* 2003a,b, Saathoff *et al* 2003 and the references therein). The role of special relativity as one of the fundamental tenets of physics is established ever more firmly by careful experimental studies such as these.

From the standpoint of testing for a photon mass, the central issue is one of searching for a frequency (or wavelength) dependence in the speed of light. As discussed above, frequency dispersion of the velocity of light is the most direct consequence of a nonzero photon mass. The investigations of invariance of c over the electromagnetic spectrum thus provide the most immediate approaches to search for some trace of the massive photon. Prior to the 1970s, c had already been measured to an accuracy of one to ten parts in 10^6 over much of the electromagnetic spectrum. However, there was no evidence in favour of a dispersion effect up to that point.

Such measurements have been made by several different approaches, and an excellent review of them was written by Froome and Essen (1969). The general conclusion was that the speed of light had been shown to remain constant over the range of frequencies from 10^8 to 10^{15} Hz within an accuracy of about one to ten parts in 10^5–10^6. According to equation (3.5), since the dispersion effect depends quadratically on wavelength (frequency), considerable overall improvement in the situation could thus be achieved by searching for dispersion at much

中国科技论文在线 http://www.paper.edu.cn

lower frequencies (or longer wavelengths), even if it must be done with less accuracy. In 1937, Ross and Slow made a determination of the phase velocity of radio waves transmitted along the surface of the ground. The average result obtained for this velocity over the wavelength range 20–120 m was 2.95×10^8 m s^{-1}, with the overall experimental uncertainty of the measurement found to be about 5%. If this deviation is ascribed to a nonzero photon mass effect on the fixed propagation path, it corresponds to $m_\gamma \leqslant 5.9 \times 10^{-42}$ g. A very comprehensive investigation of the speed of medium-band radio waves (wavelength of 230–345 m) was carried out during 1934–1935 by Mandelstam and Papalexi (1944) and their collaborators. The method comprised a determination of the time of transit of waves between sending and reflecting stations, by measuring the phase difference between two sets of waves which had frequency ratios that were rational. The phase delay of the two waves was calculable. Except for overland transmission, where the measured dispersion was quite large ($\sim$2%) due to various intervening obstacles, the mean results for the speed of the radio waves was between the limits of 2.990 and 2.995×10^8 m s^{-1} for transmission through clear air, or over sea or fresh water. When analysed in terms of a wavelength-dependence of the speed of light, their findings would place an upper limit on the photon rest mass of $m_\gamma \leqslant 5.0 \times 10^{-43}$ g. This result was improved by Al'pert *et al* (1941) who used the same technique and found $m_\gamma \leqslant 2.5 \times 10^{-43}$ g from a velocity shift of $< 7 \times 10^{-4}$ for radio waves of $300 \leqslant \lambda \leqslant 450$ m for transmission over sea water.

Using a radio-wave interferometer operating over a frequency span from 172.8 MHz to $\approx 10^{15}$ Hz, Florman (1955) measured the velocity of propagation of electromagnetic waves at the surface of the earth. Converted to the value in vacuum, the measured phase velocity was found to be $299\,795.1 \pm 3.1$ km s^{-1} with a 95% confidence interval, the uncertainty of which would reduce to ± 1.4 km s^{-1} including an estimated limit to the systematic error of ± 0.7 km s^{-1} when based on a 50% confidence interval. The measurement accuracy was limited primarily by the uncertainty within which the refractive index of air could be obtained from measured values of pressure, temperature and relative humidity. If this result is interpreted in terms of dispersion of light, the relative difference of the velocity would be $\Delta c/c \leqslant 10^{-5}$. Substituting those parameters into equation (3.5) and neglecting the higher order term, this then corresponds to an upper limit on the photon mass of $m_\gamma \leqslant 5.6 \times 10^{-42}$ g.

When the terrestrial (laboratory) conditions eventually became an obstacle to obtaining higher precision measurements on the frequency-dependence of light, astronomical observations of the dispersion of electromagnetic waves from distant sources then began to provide more promising approaches to extend the accuracy of the determinations of the relative velocities at different wavelengths. These types of measurements could well be placed in the category of extra-terrestrial observations, but we discuss them here because the same principle used in the laboratory measurements is employed. In a letter to *Nature*, Lovell *et al* (1964) analysed optical and radio events that occurred in four flare stars (UV Ceti, V371 Orionis, YCZ Mi and EV Lac.) and concluded that the velocity of light and radio waves was the same to within four parts in 10^7 over a wavelength range from 0.54 μm to 1.2 m, which led to an upper limit of $m_\gamma \leqslant 1.6 \times 10^{-42}$ g on the photon mass. The authors also introduced a parameter p to help interpret their results in terms of a linear dependence of c on wavelength λ

$$p = \frac{c}{\Delta c}\frac{\lambda_2}{\lambda_1}. \tag{4.1}$$

This made it possible to relate measurements from different regions of the spectrum that had different limits on the dispersion in velocity Δc. Their resulting value for p was 5×10^{12}, which was indeed superior to the values obtained from terrestrial measurements. For example, the corresponding value for the work of Froome (1958) was $p = 1 \times 10^{10}$ at 72 GHz, and for Florman (1955) it was $p = 3 \times 10^{11}$ at 173 MHz. However, as pointed out by Brown (1969),

中国科技论文在线 http://www.paper.edu.cn

this parametrization is not a good way to characterize the variation of speed with energy, because Δc did not approach zero as λ_1 approaches λ_2. This difficulty could be avoided by the introduction of $(\lambda_2 - \lambda_1)/\lambda_1$ in place of λ_2/λ_1 in the definition of p, as was suggested by Bay and White (1972). However, as far as the photon mass is concerned, a larger p does not mean a lower limit on the photon mass, because p is only sensitive to the ratio of different wavelengths while the photon mass is characterized not only by the wavelength ratio but more directly by the absolute magnitude. Hence, the longer wavelengths would result in a lower limit on the photon mass even if the measurement of the relative velocities is less accurate due to the quadratic dependence on wavelength, as per equation (3.5). In a succinct review, Brown (1969) clarified the statements concerning the energy-independence of the velocity of light contained in several articles (see the references therein). Brown used the parameter p to weight the experimental results from different frequency ranges. Because the range of wavelengths examined was crucial, the author argued that the wider range of energies measured in the laboratory made it possible to obtain better limits on p from those measurements than from the astronomical ones, which was in opposition to the views of Lovell *et al* (1964) and Warner and Nather (1969). Using data for waves with energies of $E = 4 \times 10^{-9}$ eV ($\lambda = 300$ m) and $E = 6$ GeV, the result was $\Delta c/c \leqslant 5 \times 10^{-4}$, implying $p > 3 \times 10^{21}$ and $m_\gamma \leqslant 2.3 \times 10^{-43}$ g. This value of p was an improvement of almost five orders of magnitude compared with the value from the observations of the Crab Nebula pulsar by Warner and Nather (1969), who found $p > 3 \times 10^{16}$ over a wavelength range of 0.35–0.55 μm, with $\Delta c/c \leqslant 5.0 \times 10^{-17}$, which set the most stringent limit on the possible speed dependence on frequency up to then, but which implied a limit on the photon mass of only $m_\gamma \leqslant 5.2 \times 10^{-41}$ g. Similarly, the data of Mandelstam and Papalexi (1944) and Luckey (1952), who measured the velocity of 170 MeV gamma rays, yields $p > 10^{18}$, implying $m_\gamma \leqslant 2.0 \times 10^{-42}$ g, as contrasted with $p > 5 \times 10^{12}$ reported by Lovell *et al* (1964). In 1973, Brown *et al* reported an experiment which directly compared the velocities of propagation of short pulses of eV (visible) and GeV electromagnetic radiation. Employing time-of-flight techniques over a flight path of 1310 m (4300 ft) and a flight time of 4.3 μs, the results gave a relative velocity difference $(c\,(\mathrm{GeV}) - c\,(\mathrm{eV}))/c\,(\mathrm{eV}) \equiv \Delta c/c = \Delta t/t = (1.8 \pm 6) \times 10^{-6}$, corresponding to $p < 10^{15}$ but a worse limit on the photon mass.

In a brief review of possible dispersion of the velocity of light in vacuum by Bay and White (1972), the authors invoked a modified Cauchy-type formula to represent the dispersion,

$$n^2 = 1 + \frac{A}{\nu^2} + B\nu^2, \tag{4.2}$$

in which n is defined by $c_{\mathrm{phase}} = c_0/n$ and c_0 is the velocity of light with frequency ν in the absence of dispersion, and the parameters A and B characterize the dispersive effect of the frequency-dependent speed of light. For compatibity with special relativity, the only possible version of this dispersion formula that could hold for vacuum required $A < 0$ and $B = 0$, in particular, $A = -(mc^2/h)^2$ with m denoting the mass of the particles. The results of several pulsar measurements interpreted according to equation (4.1) by Bay and White (1972) indicated that the speed of light was constant to within 10^{-20} throughout the visible, near infrared and ultraviolet regions of the spectrum, corresponding to a rough upper limit on the photon mass of $m_\gamma < 3 \times 10^{-46}$ g. This limit due to dispersion of the speed of light well exceeds that of any of the metrological experiments.

In 1999, Schaefer made use of explosive astrophysical events at high redshift to place strict constraints on the limits of the fractional variation in the speed of light with frequency, the photon mass and the energy scale of quantum gravity. By analysing the constraints for bursts with measured redshift from observations over the range of radio to gamma rays, two low limits on photon mass were obtained from gamma ray bursts GRB 980703 (4.2×10^{-44} g)

中国科技论文在线 http://www.paper.edu.cn

Table 1. Upper bounds on the dispersion of the speed of light in different ranges of the electromagnetic spectrum, and the corresponding limits on the photon mass.

Author (year)	Type of measurement	Wavelength (energy or frequency) range	$\frac{\Delta c}{c}$	Limits on m_γ g
Ross *et al* (1937)	Radio waves transmission overland	20–120 m	0.05	5.9×10^{-42}
Mandelstam and Papalexi (1944)	Radio waves transmission over sea	230–345 m	7×10^{-4}	5.0×10^{-43}
Al'pert *et al* (1941)	Radio waves transmission over sea	300–450 m	7×10^{-4}	2.5×10^{-43}
Florman (1955)	Radio-wave interferometer	172.8 MHz−10^{15} Hz	10^{-5}	5.7×10^{-42}
Lovell *et al* (1964)	Pulsar observations on four flare stars	0.54 μm−1.2 m	4×10^{-7}	1.6×10^{-42}
Froome (1958)	Radio-wave interferometer	72 GHz	3.3×10^{-7}	4.3×10^{-40}
Warner *et al* (1969)	Observations on Crab Nebula pulsar	0.35–0.55 μm	5.0×10^{-17}	5.2×10^{-41}
Brown *et al* (1973)	Short pulses radiation	eV–GeV	1.8×10^{-6}	1.4×10^{-33}
Bay *et al* (1972)	Pulsar emission	Microwave to ultraviolet	1×10^{-20}	3×10^{-46}
Schaefer (1999)	Gamma ray bursts (GRB980703)	5.0×10^{9}–1.2×10^{20} Hz	6.6×10^{-13}	4.2×10^{-44}
	Gamma ray bursts (GRB930229)	7.2×10^{18}–4.8×10^{19} Hz	6.3×10^{-21}	6.1×10^{-39}

and GRB 970508 (1.5×10^{-43} g). The limits on the fractional variation in the speed of light with frequency $\Delta c/c$ were 6.6×10^{-13} and 2.9×10^{-12}, respectively. The most stringent bound on $\Delta c/c$ was 6.3×10^{-21} (corresponding $p = 1.1 \times 10^{21}$) for GRB 930229, which was almost 10^4 times better than the Crab pulsar limit (Warner and Nather 1969), but only yielded an upper limit of 6.1×10^{-39} g on the photon mass due to the extra-high frequency involved.

Table 1 presents a summary of all these results for a simple comparison of the fractional variations, $\Delta c/c$, with frequency and the corresponding upper limits on the photon mass. Theoretically speaking, to obtain tighter constraints on the photon mass, one should choose waves of lower frequency that propagate over longer distances. On the other hand, very low energy waves are difficult to transmit over longer pathways because of the dissipation involved. However, for testing the energy-independence of propagating waves over a large spectral band, there is no need to use only low energies. Using the astrophysical data from high energy pulsars it is possible to search for an energy-dependence of massless particles. Hirata *et al* (1987) and Bionta *et al* (1987) detected the neutrinos from SN 1987A over the energies 10–30 MeV, yielding a limit of about $\Delta c/c \leqslant 2 \times 10^{-12}$. Through observation of the narrow phase structure of emissions from the 33 ms Crab pulsar at a range of 50–500 MeV, Thompson *et al* (1975) and Clear *et al* (1987) found a limit of $\Delta c/c \leqslant 2.5 \times 10^{-14}$. Haines *et al* (1990) analysed the observations of Hercules X-1 (Dingus *et al* 1988), the data of which spanned an energy range of 100–2000 TeV, yielding a bound on the dispersion by $\Delta c/c \leqslant 2 \times 10^{-13}$, but none of these led to improvements on the limit of the photon mass.

4.3. Null tests of Coulomb's inverse square law

4.3.1. Historical review of Coulomb's law. The famous inverse square law of electrostatics, first published in 1785 by Charles Augustin de Coulomb, carries his name and is the fundamental law governing electrostatic interactions. As the first quantitative physical

中国科技论文在线 http://www.paper.edu.cn

principle developed within electrical science, Coulomb's inverse square law has been the basis for many significant contributions to the development of electricity, magnetism and related fields. From Coulomb's law and the principle of superposition, one arrives at Gauss's law and the conservative nature of the electric field. The laws of electrostatics may be generalized using special relativity to obtain Maxwell's equations. The validity of Coulomb's law has been tested continuously over the past two centuries, particularly in its inverse square nature. Based on the classical ingenious scheme devised by Henry Cavendish (1773), modern experiments usually yield not only the result of possible deviations from true inverse square behaviour, but also upper limits on the photon rest mass, as we shall see below.

Perhaps the first investigator to explore the interaction between charges was Benjamin Franklin in 1755. In his empirical studies, he observed that when a cork ball suspended by a silk thread was placed near a charged metal cup, the cork was strongly attracted to the surface of the cup. However, when the cork was placed anywhere inside the metal cup, it was not attracted to the inside surface of the cup at all. He thought this phenomenon was inconceivable and he could not explain it. So Franklin communicated his discovery to his friend, Joseph Priestley, and expected him to perform this experiment to confirm the result. In 1766, Priestley repeated this experiment and concluded that an electrically charged cavity conductor did not produce electric force on the charges inside it. Besides this, he found another phenomenon: there was no charge on the inside surface of the cavity when the cavity was electrically charged. Priestley reported his results in 1767 in his classic treatise '*The history and present state of electricity, with original experiments*'. To suggest an explanation for this phenomenon, Priestley associated it with the contemporary findings of Newton's gravitation and made the bold deduction that the law of electric force between charges was the same as the law of gravitational attraction, i.e. it was also an inverse square law. Unfortunately, Priestley did no further research in this area.

The first experimental investigation of what was to become Coulomb's inverse square law was made in 1769 by John Robison (Elliott 1966). The experiment was very simple. The repulsive force between two charged spheres was balanced by the force of gravity acting on a pivoted arm. By adjusting the supporting beam of the pivoted arm to different angles, the repulsive force could be measured at several distances from the known weight of the balance sphere. Robison expressed his results in terms of a possible deviation from an inverse square law, postulating that the exponent applied to the charge separation distance was not exactly 2 but $2+q$. He found that the repulsive forces between two charges were inversely proportional to the distance squared between them, and that the value of q was 0.06. Robison ascribed the result to experimental error and concluded that the magnitude of the electric force between two charges was inversely proportional to the square of the distance between them. Unfortunately again, Robison did not report his experimental results until 1801. By then Coulomb had already published his own work and this inverse square law would become known as Coulomb's law. Even so, Robison's work was essential to the early theories of electromagnetism, which reached their apex in the work of Robison's fellow, James Clerk Maxwell. It was not understood that there could be other interpretations of Robison's experiment, until in the 20th century it became clear that an implied limit on the photon mass of 4×10^{-40} g could be derived from it.

In 1773, another predecessor of Coulomb in this area was Henry Cavendish, who employed concentric spheres to study the interaction between charges indirectly. The experimental apparatus is shown in figure 2, and it operated as follows. First, the globe was connected to one of the closed hemispheres by a conducting wire. Then, the outer sphere was electrically charged until the connecting wire was broken by a withdrawable silk thread. Finally, the outer sphere was opened and removed, and discharged completely. A pith-ball electrometer was then used to detect the electric charge on the inner globe. The experimental result was that the

中国科技论文在线 http://www.paper.edu.cn

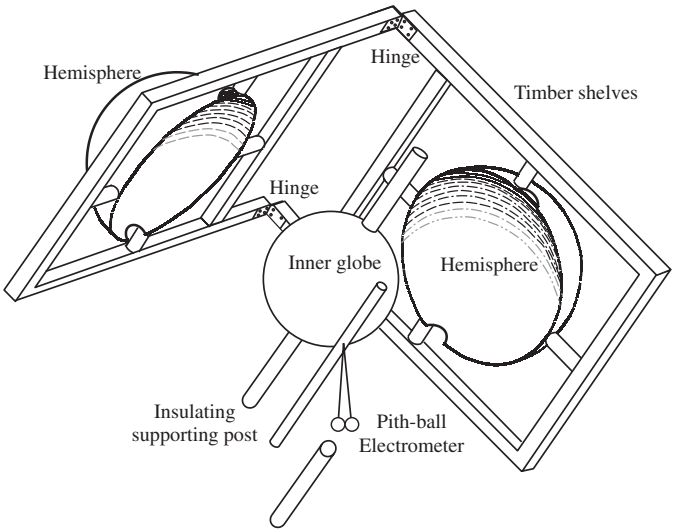


Figure 2. The Cavendish apparatus for testing the inverse square law of electrostatics. The inner globe was fixed on an insulated supporting post. The hollow pasteboard hemispheres, slightly larger than the globe, were mounted in wooden frames via two glass bars. The frames were coupled with hinges so as to close the hemispheres easily. When the frames were closed, the globe and the hemispheres formed a set of insulated concentric spheres. Both the globe and hemispheres were covered with tinfoil to make them essentially perfect conductors of electricity.

pith balls of the electrometer did not separate, and this indicated the absence of charge on the inner globe.

In explaining his result, Cavendish suggested that, as with the gravitational force between bodies, the electrical force between charges obeyed an inverse square law as well, but with the unique difference that the electric force between like charges was repulsive while that between opposite charges was attractive. The following model illuminates his reasoning. Let the electric force between charges takes the form of $F \sim r^{-n}$; then, suppose that there was an electrically charged spherical shell with a uniform surface charge density σ, and consider a unit point charge P placed inside the shell. The force acting on the point charge P would then consist of two parts: one was from the charges in the area $\mathrm{d}S_1$, which has a solid angle $\mathrm{d}\Omega_1$ towards the point charge P, while the other was from $\mathrm{d}S_2$ with solid angle $\mathrm{d}\Omega_2$ as shown in figure 3. The force acting on P from $\mathrm{d}S_2$ would be $\sigma\,\mathrm{d}S_2/r_2^n\boldsymbol{r}_0$, while the force from $\mathrm{d}S_1$ would be $-\sigma\,\mathrm{d}S_1/r_1^n\boldsymbol{r}_0$ where $\boldsymbol{r}_0$ denotes the unit vector pointing along the line of action of the force. So, the net force on the unit point charge P would be

$$\mathrm{d}\boldsymbol{F} \propto \frac{\sigma\,\mathrm{d}S_2}{r_2^n}\boldsymbol{r}_0 - \frac{\sigma\,\mathrm{d}S_1}{r_1^n}\boldsymbol{r}_0. \tag{4.3}$$

Considering the relationship between an area and corresponding solid angle, namely $\mathrm{d}\Omega_1 = \mathrm{d}S_1\cos\theta/r_1^2$, $\mathrm{d}\Omega_2 = \mathrm{d}S_2\cos\theta/r_2^2$ and $\mathrm{d}\Omega_1 = \mathrm{d}\Omega_2 = \mathrm{d}\Omega$, it would then be easy to get the net force on the unit charge P due to the surface charge densities in the areas $\mathrm{d}S_1$ and $\mathrm{d}S_2$, namely

$$\mathrm{d}\boldsymbol{F} \propto \frac{\sigma\,\mathrm{d}S_2}{r_2^n}\boldsymbol{r}_0 - \frac{\sigma\,\mathrm{d}S_1}{r_1^n}\boldsymbol{r}_0 = \frac{\sigma\,\mathrm{d}\Omega}{\cos\theta}\left(\frac{1}{r_2^{n-2}} - \frac{1}{r_1^{n-2}}\right)\boldsymbol{r}_0. \tag{4.4}$$

Obviously, if $n = 2$, the charges on $\mathrm{d}S_1$ and $\mathrm{d}S_2$ had a null net force on the charge P, which indicated that the force acting on the charge inside the electrically charged spherical shell was

中国科技论文在线 http://www.paper.edu.cn

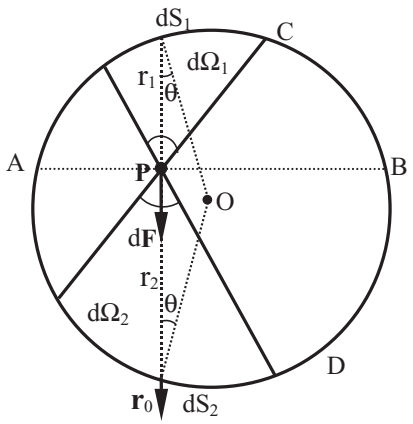


Figure 3. The electrical force was inversely proportional to the square of the distance. The electrically charged metal spherical shell was divided into two parts by the plane AB. A point charge P was placed inside the shell, which experienced a force from the charge on the surface of the shell. Although the upper part, ACB, was smaller than the bottom part, ADB, the net force acting on the charge P will be exactly zero if the electric force obeys the inverse square law.

exactly zero if the electric force obeyed the inverse square law. In other words, the uniformly distributed charge on the outer surface of the metal sphere was the necessary consequence of an inverse square law of electric charges. So, if there was any deviation from the inverse square law, charges would migrate through the wire to the inner globe in Cavendish's experiment. If $n > 2$, the action from the lower hemisphere would exceed that from the upper one, which would result in the point charge P moving upwards. Whereas, if $n < 2$, then, the point charge P would move downwards. Cavendish likewise interpreted his findings in terms of a possible breakdown of the inverse square law, and concluded that the deviation q in the exponent of r cannot be greater than 0.02. Modern interpretations of Cavendish's result now give an upper limit on the photon rest mass that was a little greater than 1×10^{-40} g. Obviously, the large background electric fields that arose when the two outer hemispheres were removed would produce the major limitation to the accuracy of this experiment, and an unavoidable result of this design was that stray charges could leak to the inner sphere along the insulators supporting it. Like Robison, Cavendish did not publish his discovery but instead, about 100 years later, Maxwell mentioned the experiment in his book '*The Electrical Researches of the Honourable Henry Cavendish*'.

In 1873, a revised version of Cavendish's experiment was performed by Maxwell at the Cavendish Laboratory in Cambridge University. The main measure used to improve the experimental embodiment was that the outer sphere was earthed during the second part of the experiment instead of being removed, thus providing a perfect shield for disturbances, but at the expense of determining the potential of the inner shell with greater difficulty. Maxwell employed a spherical air condenser consisting of two insulated spherical shells, the outer one having a small hole in it so that the inner one could be tested for charge by inserting an electrode from a Thomson electrometer. The hole was closed by a small lid carrying an inward probe which simultaneously connected the two shells together. It was imperative that the surface of the outer conductor be a closed one during the first part of the experiment. Then, the outer shell was charged to a high potential, and the lid and the connector were removed by a silk thread. Finally, Maxwell observed the same experimental phenomenon as Cavendish and concluded that the deviation q was less than 5×10^{-5}, now interpreted as corresponding to an upper limit on the photon mass of 5×10^{-42} g.

中国科技论文在线 http://www.paper.edu.cn

Although numerous workers had investigated the force law between charges before Coulomb, and some had even attained higher precision, it was Coulomb who first proclaimed the inverse square law, in 1785. A noteworthy point that should be emphasized was that the experiments performed by Coulomb were done independent of those of all others. The experiments were divided into two steps (Elliott 1966). Using a torsion balance Coulomb demonstrated directly that two like charges repel each other with a force that varies inversely with the square of the distance between them. Then, the law of attraction between unlike charges was indirectly demonstrated through what was thought to be an improperly functioning torsion balance, although Coulomb did write in his memoirs that he in fact had been able to test the law between unlike charges by use of the torsion balance. From his results, which are widely discussed in many books and reviews, Coulomb unequivocally established the distance dependence of the electric force.

During the next 40 years after the publication of Coulomb's memoirs on electrostatics, his findings were strongly disputed (Heering 1992), especially in Germany. The main reason for this was that his inverse square law happened to take the same form as Newton's inverse square law of gravitation. Several critical physicists, such as Simon, Volta and Oersted, raised strong opposition to Coulomb's law. The experiments Coulomb claimed to have performed successfully in his memoirs were repeated, but none of Coulomb's contemporaries succeeded in reproducing his results. Some then preferred to believe that Coulomb did not actually arrive at the inverse square law via a series of doubtful measurements made with his torsion balance, but instead developed it only from theoretical considerations. There were then attempts to replace Coulomb's relationship with alternative formulations, but eventually the true inverse square nature of the electrostatic force became generally accepted and posterity has given it his name.

4.3.2. General method and technical background. The distance dependence of the electrostatic force was expressed quantitatively by Cavendish and Coulomb in terms of the inverse square law. Through Gauss's law and the divergence theorem, this law leads to the first of Maxwell's equations, which defines the relationship between the electric field and local charge density. However, if the photon has mass, an additional term is required which changes Maxwell's equations to those of Proca. From the time of Cavendish onwards, Coulomb's inverse square law was tested in novel experiments employing ever more sophisticated techniques. As a result, methods of finding deviations from Coulomb's inverse square law via laboratory methods subsequently set the most precise bounds on the size of the photon mass as compared to other larger-scale methods. The original experiments had an accuracy of only a few per cent and were of laboratory scales of length. Experiments with higher precision and involving a wider range of lengths were then performed thereafter (Goldhaber and Nieto 1971b, 1976). It is now customary to quote the tests of the inverse square law in one of the following two ways (Jackson 1975):

(a) Assume that the force varies with the distance r between two point charges as per the phenomenological formulation $r^{-2\pm q}$, and quote a value or limit for q which represents the departure from exact inverse square law behaviour.

(b) Assume that the electrostatic potential has the 'Yukawa' form $r^{-1}\exp(-\mu_\gamma r)$ instead of the simple Coulomb form r^{-1}, and quote a value or limit for μ_γ or μ_γ^{-1}. Since $\mu_\gamma = m_\gamma c/\hbar$, tests of the inverse square law are often then expressed directly in terms of an upper limit on the photon rest mass. The results of geomagnetic and extra-terrestrial experiments are typically also given in terms of μ_γ or m_γ, while laboratory experiments are often interpreted in terms of both q and μ_γ or m_γ.

中国科技论文在线 http://www.paper.edu.cn

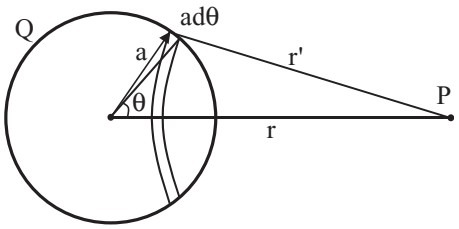


Figure 4. A uniformly charged spherical shell is broken into rings for obtaining the electrostatic potential at point P, which is located a distance r from the centre of the shell. A total charge Q resides on the spherical shell of radius a.

Experimental studies of the photon rest mass or, equivalently, searches for deviations from Coulomb's law are to some extent made difficult because, for an experiment confined to dimension D, the effects of finite μ_γ are of the order $(\mu_\gamma D)^2$, as propounded in a theorem proposed by Goldhaber and Nieto (1971b). This means that an experiment designed to find the effects of a massive photon or of a breakdown of Coulomb's law must either interrogate a region of size comparable to μ_γ^{-1} or it must have extraordinary precision to detect the otherwise infinitesimal evidence of photon mass or such a deviation. The concentric sphere experiments originated by Cavendish, which are the typical apparatus used frequently by his successors, exemplify the progress made in increasing the detectability of weak signals using apparatus with enormous sensitivity, which has been achieved through technological development. The principal advantage of this method is that all the parameters involved can be individually varied and tested, whereas astronomical methods usually involve a number of factors that are subject to assumptions and interpretations that are difficult to verify.

4.3.3. Static experiments. The original concentric spheres experiment performed by Cavendish in 1773 gave an upper limit on q of $|q| \leqslant 0.02$, and this result was improved to $|q| \leqslant 5 \times 10^{-5}$ in 1873 by Maxwell. The corresponding limits on the photon rest mass are 1×10^{-40} g and 5×10^{-42} g, respectively, as was mentioned above. In these experiments the electric potential on the inner conducting sphere was measured. From the value of this potential and the relation between q and the potential, Maxwell (1873) first derived expressions for the size of possible deviations from pure inverse square behaviour, and a more detailed attempt at this task was undertaken much later by Fulcher and Telljohann (1976) and by Fulcher (1986), the results of which then became the general frame of reference for later interpretation of similar laboratory experiments (Zhang 1998). In what follows, we will briefly deduce the electrostatic potential of a uniformly charged spherical shell, and then from this deduction, we will show how the potential difference of two or more concentric spherical shells can be obtained.

Suppose that the electrostatic force between two unit charges is an arbitrary function $F(r)$ of the distance r between them. The electrostatic potential is given by

$$U(r) = \int_r^\infty F(s)\,\mathrm{d}s. \tag{4.5}$$

Now, consider a uniform distribution of charge Q over a spherical shell of radius a and break the spherical shell into rings of thickness $a\,\mathrm{d}\theta$, as shown in figure 4. Then, the differential element of charge for a chosen ring is given by $\mathrm{d}q = (Q/4\pi a^2) \cdot 2\pi a^2 \sin\theta\,\mathrm{d}\theta = (Q/2)\sin\theta\,\mathrm{d}\theta$, which produces the potential $\mathrm{d}V = (Q/2)\sin\theta\,\mathrm{d}\theta U(r')$ at point P with an interval r' between the corresponding rings. As shown in figure 4, we have the relation: $r'^2 = r^2 + a^2 - 2ar\cos\theta$,

中国科技论文在线 http://www.paper.edu.cn

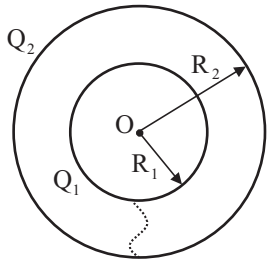


Figure 5. A model of two concentric spherical shells used in Cavendish type experiments for testing Coulomb's inverse square law. A charge Q_1 resides uniformly on the inner shell, which has radius R_1, and a charge Q_2 is on the outer shell, of radius R_2.

then $r'\,\mathrm{d}r' = ar\sin\theta\,\mathrm{d}\theta$. So the potential at a distance r from the centre of the shell is readily determined as

$$V(r) = \int \frac{Q}{2}\sin\theta\,\mathrm{d}\theta U(r') = \frac{Q}{2ar}[f(r+a) - f(|r-a|)], \tag{4.6}$$

where

$$f(r) \equiv \int_0^r sU(s)\,\mathrm{d}s. \tag{4.7}$$

Let us then apply these expressions to the experiments of Cavendish type, and suppose that the radii of the two concentric spheres are R_1 and R_2 ($R_1 < R_2$) with charges Q_1 and Q_2 spread uniformly over them, respectively (as shown in figure 5). Using equation (2.6), one finds the potential on the inner shell to be

$$V(R_1) = \frac{Q_1}{2R_1^2}f(2R_1) + \frac{Q_2}{2R_1R_2}[f(R_1+R_2) - f(R_2-R_1)], \tag{4.8}$$

while the potential on the outer shell is

$$V(R_2) = \frac{Q_2}{2R_2^2}f(2R_2) + \frac{Q_1}{2R_1R_2}[f(R_1+R_2) - f(R_2-R_1)]. \tag{4.9}$$

After charging the outer shell to a potential of V_0, a part of the charge would pass through the connecting wire to the inner shell until an equilibrium of $V(R_1) = V(R_2) \equiv V_0$ was reached. Then, the charge accumulated on the inner shell can be found from equations (4.8) and (4.9) as

$$Q_1 = 2R_1V_0\frac{R_1f(2R_2) - R_2[f(R_1+R_2) - f(R_2-R_1)]}{f(2R_1)f(2R_2) - [f(R_2+R_1) - f(R_2-R_1)]^2}. \tag{4.10}$$

If Coulomb's law is correct, the electric potential has the form of $U(r) = r^{-1}$; hence $f(r) \equiv r$. Because the two shells had been connected by a conducting wire, the charge originally given to the inner shell will end up at the outer surface of the outer one, i.e. $Q_1 = 0$, which is the natural consequence of Coulomb's r^{-2} law. Actually, for a conductor of arbitrary shape, the charge distribution is so arranged that the electric field inside the conductor vanishes, and the time constant to establish electrostatic equilibrium is very short (of the order of 10^{-19} s). The aim of experimental verifications of Coulomb's law is to find traces of the residual fields between the shells.

In the Cavendish experiment, after the two shells were charged and the interconnection was broken, the outer shell was removed to infinity. According to equations (4.8) and (4.10), the potential of the inner shell would then be

$$V_{\mathrm{C}}(R_1) = \frac{Q_1}{2R_1^2}f(2R_1). \tag{4.11}$$

中国科技论文在线 http://www.paper.edu.cn

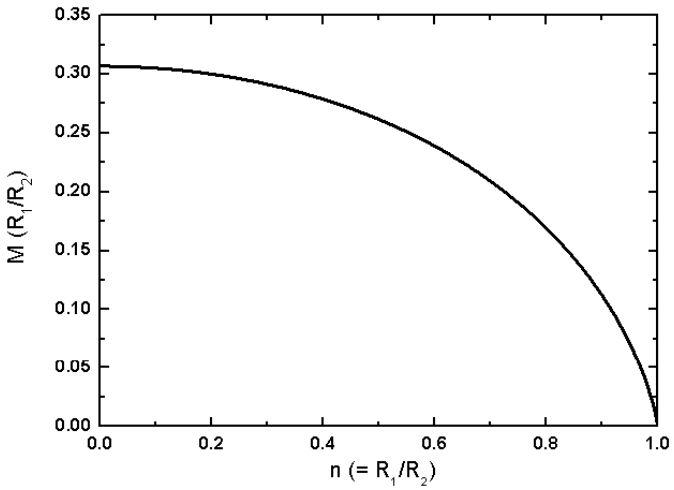


Figure 6. The geometrical factor $M(R_1, R_2)$ for concentric spherical shells varies monotonically with the ratio of the radii, R_1/R_2 ($R_1 < R_2$), and has its extremum at $M_{\max}$ $(R_1/R_2 = 0) = 0.3069$ and $M_{\min}$ $(R_1/R_2 = 1) = 0$.

In Maxwell's case, after the interconnection was broken, the outer shell was then earthed instead of being taken away, which meant $V(R_2) \equiv 0$. So with the help of equations (4.8)–(4.10), the potential on the inner shell could then be expressed as

$$V_{\mathrm{M}}(R_1) = V_0 \left[1 - \left(\frac{R_2}{R_1} \right) \frac{f(R_2 + R_1) - f(R_2 - R_1)}{f(2R_2)} \right]. \tag{4.12}$$

Following Maxwell, suppose that the exponent in Coulomb's inverse square law is not 2 but $2 + q$ with $|q| \ll 1$. In that case, for a unit point charge, we have

$$U(r) = \frac{1}{1+q} \frac{1}{r^{1+q}} \approx \frac{1}{r^{1+q}} \tag{4.13}$$

and to first order in q,

$$f(r) \approx r(1 - q \ln r). \tag{4.14}$$

Substituting (4.14) in (4.11) and (4.12), the link between the potential and the deviation q would arise from the following formulae in the experiments of Cavendish and Maxwell, respectively:

$$V_{\mathrm{C}}(R_1) \approx \left(\frac{R_2}{R_2 - R_1} \right) q V_0 M(R_1, R_2), \tag{4.15}$$

$$V_{\mathrm{M}}(R_1) \approx q V_0 M(R_1, R_2), \tag{4.16}$$

where $M(R_1, R_2)$ is a dimensionless geometrical parameter of order unity and its characteristic curve is shown in figure 6, and

$$M(R_1, R_2) = \frac{1}{2} \left[\frac{R_2}{R_1} \ln \frac{R_2 + R_1}{R_2 - R_1} - \ln \frac{4R_2^2}{R_2^2 - R_1^2} \right]. \tag{4.17}$$

Obviously, if $q = 0$, the potential of the inner sphere is also zero, which is the case predicted by Coulomb's inverse square law. So, by detecting the potential on the inner shell directly, one could obtain the deviation from Coulomb's inverse square law.

The main hindrance to further improvement in static experiments of this type are contact potentials (Camp *et al* 1991). Contact potential is an electrostatic potential difference between

中国科技论文在线 http://www.paper.edu.cn

two metals caused by their different work functions, which are the energies needed to remove an electron from the metal (Michaelson 1977). In some modern precision experiments, such as measurements of the Casimir force, contact potentials have generally been proven to be of the order of several millivolts for dissimilar metals or coated metal media (Bordag *et al* 2001), and in the worst case, even up to a 'shockingly large' value of 430 mV (Lamoreaux 1997). This problem no doubt arose in the experiments of Cavendish and Maxwell, as they used contacting leads to measure the potential at different points on the shells. This problem is overcome in dynamic experiments by measuring the potential *difference* instead of the potential itself.

4.3.4. Dynamic experiments. In order to obtain a higher precision, modern experiments using the concentric shell arrangement of Cavendish were carried out with high voltage ac signals applied to the outer shell and with phase-sensitive detection used to sense the relative potential difference between the shells. Moreover, the motivation for concentric-shell experiments had by then become predominated mainly by interest in the photon rest mass as opposed to simply testing the exactness of the inverse square law. For this type of experiment, the relative difference of potential between the two spheres, according to equations (4.6) and (4.14), can be expressed as

$$\frac{V(R_2) - V(R_1)}{V(R_2)} = qM(R_1, R_2), \tag{4.18}$$

where the geometrical factor $M(R_1, R_2)$ is the same, so that q is essentially the quotient of the measured potential difference $V(R_2) - V(R_1)$ and the applied voltage $V(R_2)$. With the expected relation between the potential difference and the deviation q the next step is one of finding the link between μ_γ and the potential difference.

Consider an idealized geometry of two uncharged, concentric, conducting spherical shells of radii R_1 and $R_2 (R_1 < R_2)$ with an inductor across this spherical capacitor. An alternating potential of $V_0 \exp(i\omega t)$ is then applied to the outer shell so that $V(R_2) = V_0 \exp(\mathrm{i}\omega t)$. For this case, a solution to the massive photon electromagnetic field equation (2.5) can be written as $\phi(r, t) = \phi(r) \exp(\mathrm{i}\omega t)$ and the wave equation reduces to

$$(\nabla^2 + k^2)\phi(r) = 0, \tag{4.19}$$

where

$$k^2 = \frac{\omega^2}{c^2} - \mu_\gamma^2. \tag{4.20}$$

With the proper boundary conditions, the exact result for the potential is

$$\phi(r) = V_0 \frac{R_2}{r} \frac{\mathrm{e}^{\mathrm{i}kr} - \mathrm{e}^{-\mathrm{i}kr}}{\mathrm{e}^{\mathrm{i}kR_2} - \mathrm{e}^{-\mathrm{i}kR_2}} \qquad (r \leqslant R_2). \tag{4.21}$$

Choosing a spherical Gaussian surface of radius r between the two shells and then using equation (4.21) for the interior region, the closed integral of the Proca equation (2.7) over the volume from the interior to the Gaussian surface becomes

$$\int \mathrm{d}V \nabla \cdot \boldsymbol{E} = -\mu_\gamma^2 \int \mathrm{d}V \cdot \phi(r). \tag{4.22}$$

Given this, a complete solution for the field inside a uniformly charged single sphere of radius R_2 can then be written as

$$\boldsymbol{E}(r, t) = \frac{\mu_\gamma^2}{k^2 r^2} \frac{V_0 R_2}{\mathrm{e}^{\mathrm{i}kR_2} - \mathrm{e}^{-\mathrm{i}kR_2}} [\mathrm{i}kr(\mathrm{e}^{\mathrm{i}kr} + \mathrm{e}^{-\mathrm{i}kr}) - (\mathrm{e}^{\mathrm{i}kr} - \mathrm{e}^{-\mathrm{i}kr})]\mathrm{e}^{\mathrm{i}\omega t} \cdot \frac{\boldsymbol{r}}{r}. \tag{4.23}$$

中国科技论文在线 http://www.paper.edu.cn

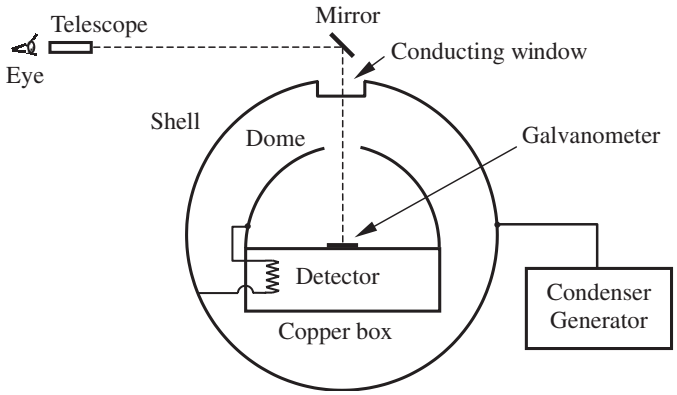


Figure 7. Experimental arrangement used by Plimpton and Lawton in 1936 for testing the inverse square law of the force between charges. The outer shell was formed from two approximately hemispherical shells, while the inner one consisted of a (lower) copper box containing the detector and a hemispherical dome above it. A specially designed condenser generator generated a 3000 V signal, which was applied to the outer shell. Any movement of the galvanometer is monitored by the mirror and the telescope through the conducting window.

A power series expansion of the electric field for $kr < 1$ and $\omega > \mu_\gamma c$ yields

$$\boldsymbol{E}(r,t) = -\frac{1}{3}\mu_\gamma^2 r V_0 \mathrm{e}^{\mathrm{i}\omega t}\left(1 - \frac{1}{10}k^2r^2 + \frac{1}{6}k^2R_2^2 - \cdots\right)\frac{\boldsymbol{r}}{r}. \tag{4.24}$$

The higher-order terms can be neglected for these experiments, and the above electric field can then be written as

$$\boldsymbol{E}(r,t) \approx -\frac{1}{3}\mu_\gamma^2 r V_0 \mathrm{e}^{\mathrm{i}\omega t}\frac{\boldsymbol{r}}{r}, \tag{4.25}$$

which indeed leads to $\nabla \times \boldsymbol{E} = 0$, and hence $\oint \boldsymbol{E}\cdot \mathrm{d}\boldsymbol{l} = 0$. With this, the potential difference between the inner and outer shells becomes,

$$V(R_2) - V(R_1) = \int_{R_1}^{R_2} \boldsymbol{E}\cdot d\boldsymbol{l} = -\frac{1}{6}\mu_\gamma^2(R_2^2 - R_1^2)V(R_2) \tag{4.26}$$

and the relative potential difference between the two spheres is

$$\frac{V(R_2) - V(R_1)}{V(R_2)} = -\frac{1}{6}\mu_\gamma^2(R_2^2 - R_1^2). \tag{4.27}$$

This result demonstrates clearly that the relative potential difference $\Delta V/V$ is independent of the frequency of the applied alternating voltage, i.e. the boundary condition problems in the dynamic experiments are the same as those in the static experiments. A second look at equation (4.27) hints that the quadratic dependence of the potential difference on μ_γ makes this method rather insensitive to small values of μ_γ.

The first dynamic experimental test of Coulomb's law can be dated back to Plimpton and Lawton (1936). The concentric shell electrostatic experiments of Cavendish and Maxwell were replaced by a quasi-static method, in which the problems due to spontaneous ionization and contact potentials were overcome by placing the detector inside the inner sphere and connecting it permanently so as to detect any change in the potential of the inner sphere relative to the outer one (as shown in figure 7). The detector was a resonance electrometer operating at a frequency of $\approx$2 Hz, which led to improved sensitivity and to reduced inductive effects which had arisen by simply opening and closing the circuits for the applied voltage on the outer

中国科技论文在线 http://www.paper.edu.cn

globe. The resonant motion of the galvanometer was produced by the potential difference between the outer globe and inner dome of the apparatus, and this motion could be observed via a mirror and telescope, which monitored it through a conducting window at the top of the outer globe. The conducting window, claimed by Plimpton and Lawton to be essential to the success of the method, was a glass-bottomed vessel threaded into the outer globe such that its surface was flush with the top surface of the outer globe. It contained a solution of ordinary salt in water. A disc of fine wire gauze covered the glass and was soldered to the threaded rim of the vessel, thus improving the electrical conductivity of this window. A harmonically alternating potential of about 3000 V, produced by a specially designed condenser generator operating at the low resonance frequency of the galvanometer, was applied to the outer globe. Tests were then made to detect the change in the potential of the dome relative to the outer globe. The results showed that no change in the thermally driven motion of the galvanometer could be detected during the course of the experiment, at a detector sensitivity of 1 μV. The radii of the two globes were 0.76 m (2.5 ft) and 0.61 m (2.0 ft), respectively. Substitution of the experimental parameter into the equations (4.18) and (4.27) then yielded a limit on the size of the deviation from Coulomb's inverse square law of $q < 2 \times 10^{-9}$ and a corresponding limit on the photon rest mass of $m_\gamma < 3.4 \times 10^{-44}$ g.

Cochran and Franken (1968) employed concentric cubical conductors instead of concentric spheres due to the cost and awkwardness of constructing and using large spheres. The most significant improvement in their experiment, compared with that of Plimpton and Lawton, was the application of a lock-in amplifier for detecting minute potential differences between the conducting surfaces. The sensitivity of their system was such that they could see changes in amplitude of 2×10^{-9} V. A signal of $\approx$1200 V ac with frequencies ranging from 100 to 500 Hz was applied to the outer box. The authors quoted two values for the deviation q from exact inverse square law behaviour. The first bound was derived from the worst-case error limit, $|q| < 4.6 \times 10^{-11}$, and the second was for the case of a probable error of 70%, $|q| < 9.2 \times 10^{-12}$. The latter gave a corresponding bound of $m_\gamma \leqslant 3 \times 10^{-45}$ g on the photon rest mass. The complicated calculations arising from the cubical configuration of the apparatus makes analysis of this experiment difficult.

An improvement to the experiment of Plimpton and Lawton was reported by Bartlett and Phillips (1969) and Bartlett *et al* (1970). Instead of two concentric spheres, their approach adopted five concentric spheres in order to improve the sensitivity and to help eliminate errors introduced by stray charges. The voltage was applied between the two outermost shells, and the induced signal between the two innermost shells was then measured. The middle one served as a shield. A potential difference of 40 kV at 2500 Hz was used between the two outer spheres. A lock-in detector with a sensitivity of $\approx$0.2 nV served to measure the potential difference between the two inner spheres. They arrived at a final result of $|q| \leqslant 1.3 \times 10^{-13}$, with the associated limit on the photon rest mass being $m_\gamma \leqslant 3 \times 10^{-46}$ g.

The experiment of Williams *et al* (1970, 1971) was designed to operate at exceptionally high sensitivity. A diagram of the apparatus is shown in figure 8. It consisted of five concentric icosahedrons. The two outermost shells were charged by 10 kV at 4 MHz; the inner shell was $\approx$1.5 m thick. A battery-powered lock-in amplifier with a detection sensitivity of $\approx 10^{-12}$ V was employed to continuously detect the line integral of the electric field between the two innermost shells. Three sets of optical fibres were used to convey the data through small apertures in the icosahedrons. In order to prevent penetration of external fields through these holes, the fibres served as waveguides, with their diameters being smaller than the cutoff frequency. The middle shell also served to reduce the effects of stray electric and magnetic fields. To ensure that the system functioned properly, optical calibration signals were periodically introduced as tests. The high frequencies used in this experiment were chosen to

中国科技论文在线 http://www.paper.edu.cn

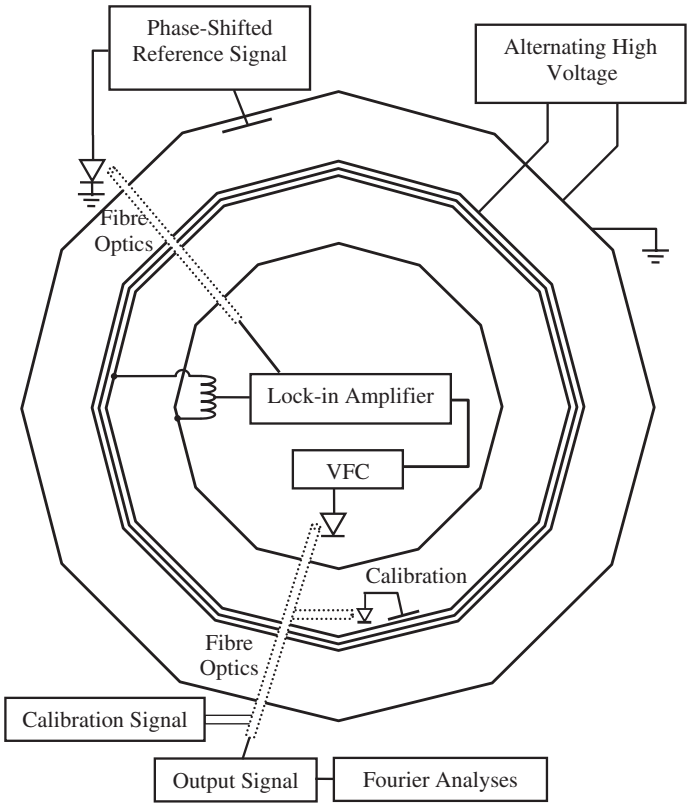


Figure 8. Experimental arrangement used by Williams *et al* in 1971 at Wesleyan University. An ac signal of 10 kV peak-to-peak at 4 MHz was applied across the two outer shells, which along with a high-Q water-cooled coil, formed a resonant circuit. A battery-powered lock-in amplifier, located inside the innermost shell, was used to search for any trace of this signal appearing across the two inner shells. Three sets of optical fibres were used for transmitting the data, which consisted of the reference signal for the phase detector, the output of the voltage-to-frequency converter (VFC) from the lock-in amplifier and a calibration voltage that was introduced periodically into the system. The output signal was analysed for evidence of a violation of Coulomb's law, which would have been the signature of a photon mass.

reduce the skin depth effects, which vary as $\delta \propto \omega^{-1/2}$. Three-day data series yielded results that were statistically consistent with the assumption that the photon rest mass is identically zero. Expressing the results as a deviation from Coulomb's law in the form of r^{-2-q}, they found $q \leqslant (2.7 \pm 3.1) \times 10^{-16}$ and the limit on the photon rest mass was $m_\gamma \leqslant 1.6 \times 10^{-47}$ g. This experiment also ruled out a theoretically predicted value for the deviation of Coulomb's law suggested by Zygan (1970a,b).

The most recent Coulomb null experiment using a principle similar to these was proposed in 1982 by Crandall, who designed the experiment such that it could be carried out by physics students at several different college levels, thus allowing for the apparatus to be improved gradually with each class. The main difference between this and earlier experiments was the use of a three-shell arrangement instead of five, with the geometry optimized for use in this kind of teaching-tool arrangement. The radii of the three icosahedral shells were 0.2, 0.5 and 1.0 m. In this arrangement, the 500 V peak-to-peak signal was applied to the two *innermost* shells at a frequency of 500 kHz. Crandall and his collaborators obtained improved results with this

中国科技论文在线 http://www.paper.edu.cn

Table 2. Results of experimental tests of Coulomb's law and the photon rest mass.

Author (year)	Experimental scheme	Deviation q	Limits on m_γ g
Robison (1769)	Gravitational torque on a pivot arm	6×10^{-2}	4×10^{-40}
Cavendish (1773)	Two concentric metal shells	2×10^{-2}	1×10^{-40}
Coulomb (1785)	Torsion balance	4×10^{-2}	$\sim 10^{-39}$
Maxwell (1873)	Two concentric shells	5×10^{-5}	1×10^{-41}
Plimpton and Lawton (1936)	Two concentric shells	2×10^{-9}	3.4×10^{-44}
Cochran and Franken (1967)	Concentric cubical conductors	9.2×10^{-12}	3×10^{-45}
Bartlett *et al* (1970)	Five concentric shells	1.3×10^{-13}	3×10^{-46}
Williams *et al* (1971)	Five concentric icosahedrons	$(2.7 \pm 3.1) \times 10^{-16}$	1.6×10^{-47}
Fulcher (1985)	Improved result for Williams' experiment	$(1.0 \pm 1.2) \times 10^{-16}$	1.6×10^{-47}
Crandall (1983)	Three concentric icosahedrons	6×10^{-17}	8×10^{-48}
Ryan *et al* (1985)	Cryogenic experiment		$(1.5 \pm 1.4) \times 10^{-42}$

approach, finding $q \leqslant 6 \times 10^{-17}$ for the deviation from Coulomb's law and $m_\gamma \leqslant 8 \times 10^{-48}$ g for the photon rest mass.

4.3.5. Other experiments. In 1985, a very different method of searching for the photon mass via Coulomb's law was developed for use at a temperature of 1.36 K by Ryan *et al* (1985). The idea underlying this search for the photon mass was that the particle was massless above a critical temperature but would acquire a mass below this temperature. Their null result established that the photon at 1.36 K had a mass of less than $(1.5 \pm 1.4) \times 10^{-42}$ g. Although this was not as low a limit as had been found in some of the other experiments, it was a unique contribution because of the low temperature ranges involved.

The results of all the experiments in this class of tests of Coulomb's law are listed in table 2, for ease of comparison. Because Coulomb's law is so fundamental to electromagnetism it is always of interest to improve the limits over which it is known to hold. The experimental results discussed above reveal that the validity of its inverse-square nature is unassailable at the macroscopic level, and as we shall see later in the review, it is known to hold over distances ranging up to 10^{13} cm. In the microscopic regime, the well-known Rutherford experiments on the scattering of alpha particles by thin metal foil gave early indications that Coulomb's law is valid at least down to distances of about 10^{-11} cm, nearly the size of the nucleus. Modern high energy experiments on the scattering of electrons proved that Coulomb's inverse square law holds even down to the Fermi scale (Breton *et al* 1991). When viewed collectively, the evidence from all these experimental results shows that Coulomb's law is valid from the macroscopic to the quantum domains, a range covering roughly 26 orders of magnitude in distance. While this represents an impressive scale by any measure, it is nevertheless still finite, and no doubt others will work to extend it.

4.4. Tests of Ampère's law

According to the Proca equations, if the photon rest mass is different from zero, not only electrostatic fields but also magnetostatic fields take on the character of exponential decay and vanish at distances of the order of μ_γ^{-1}, in contrast to the cases where they would extend to infinity, as in Maxwell's electrodynamics. A null experiment that served as a laboratory test of Ampère's law was carried out by Chernikov *et al* in 1992, and it is of interest in that regard.

中国科技论文在线 http://www.paper.edu.cn

In the case of a nonzero photon mass, and in the quasi-static limit, the magnetic field obeys the relation

$$\nabla \times \boldsymbol{B} = \mu_0 \boldsymbol{J} - \mu_\gamma^2 \boldsymbol{A}. \tag{4.28}$$

Their experimental test of Ampère's law was based on a measurement of the line integral of $\boldsymbol{B}$ along a closed curve C, which, in the case of $m_\gamma \neq 0$, becomes

$$\oint \boldsymbol{B} \cdot \mathrm{d}\boldsymbol{l} = \mu_0 \int_C \boldsymbol{J} \cdot \mathrm{d}\boldsymbol{f} - \mu_\gamma^2 \int_C \boldsymbol{A} \cdot \mathrm{d}\boldsymbol{f}. \tag{4.29}$$

So, if one chose a coil configuration for which no current passes through a surface bounded by the closed curve C, there would automatically be a null result if Ampère's law were indeed valid. Using a very sensitive superconducting quantum interference device (SQUID) as a magnetometer (Gerber *et al* 1993) to detect changes of magnetic flux at low temperatures (1.24 K), Chernikov *et al* found no distinct magnetic-flux change that could account for a photon mass. The experimental result was $m_\gamma \leqslant (8.4 \pm 0.8) \times 10^{-46}$ g, which was a limit that was substantially less stringent than those derived from the null tests of Coulomb's law, but nevertheless of interest because it was obtained via a different physical approach. Moreover, since large-scale investigations of magnetostatic phenomena usually involve astronomical observations, which will be discussed in the next section, a laboratory experiment of this type is particularly helpful in establishing range-related limits.

4.5. Torsion balance methods

The application of torsion balance techniques for detecting the photon mass was proposed in 1998 by Lakes. In a Proca field, the potentials themselves have physical significance, instead of just their derivatives. The large cosmic magnetic vector potential, $\boldsymbol{A}$, described by the Proca equations is observable since the potential acquires an energy density $\mu_\gamma^2 \boldsymbol{A}_2/\mu_0$. Lakes (1998) reported an experimental approach based on a modified Cavendish balance to evaluate the product of photon mass squared and the ambient cosmic magnetic vector potential. The basic idea was to generate a magnetic-dipole vector-potential moment $\boldsymbol{a}_\mathrm{d}$ via a suspended toroidal coil. This moment interacts with the ambient cosmic magnetic vector potential to produce a torque $\tau = \boldsymbol{a}_\mathrm{d} \times \mu_\gamma^2 \boldsymbol{A}$ on the torsion balance. The component along with the fibre (i.e. along the z direction in the laboratory frame) can be written as follows (Luo *et al* 2000, 2003):

$$\tau_z = A\mu_\gamma^2 a_\mathrm{d}(\cos\theta \cos\theta_\mathrm{A} \cos\lambda - \cos\theta \sin\theta_\mathrm{A} \sin\Omega t \sin\lambda - \sin\theta \sin\theta_\mathrm{A} \cos\Omega t), \tag{4.30}$$

where θ is the angle between the latitude and $\boldsymbol{a}_\mathrm{d}$ in the laboratory frame, θ_A the angle between $\boldsymbol{A}$ and the Earth's rotation axis, λ the latitude and Ω the rotation frequency of the Earth. The contribution to the magnetic vector potential from sources outside the solar system, within the laboratory frame of reference, will vary sinusoidally with time, one cycle per sidereal day, as a result of the rotation of the Earth. This was the case considered by Lakes, and he found a limit of $\mu_\gamma^2 A < 2 \times 10^{-9}\,\mathrm{T\,m\,m^{-2}}$, with a corresponding limit on the photon mass of 2×10^{-50} g, for an ambient magnetic vector potential of $A \approx 10^{12}$ Tm due to cluster-level fields. However, if $\sin\theta_\mathrm{A} = 0$, which would mean that the cosmic ambient vector potential is fortuitously aligned with the Earth's rotational axis, then this approach would fail.

An improved experiment, designed to overcome the direction dependence of the torsion balance method, was performed by Luo *et al* in 2002. A schematic diagram of the rotating torsion balance system used in it is shown in figure 9. In this experiment, the motion of the torsion balance is modulated by a turntable rotating at an angular frequency ω (let $\theta = \omega t$ in

中国科技论文在线 http://www.paper.edu.cn

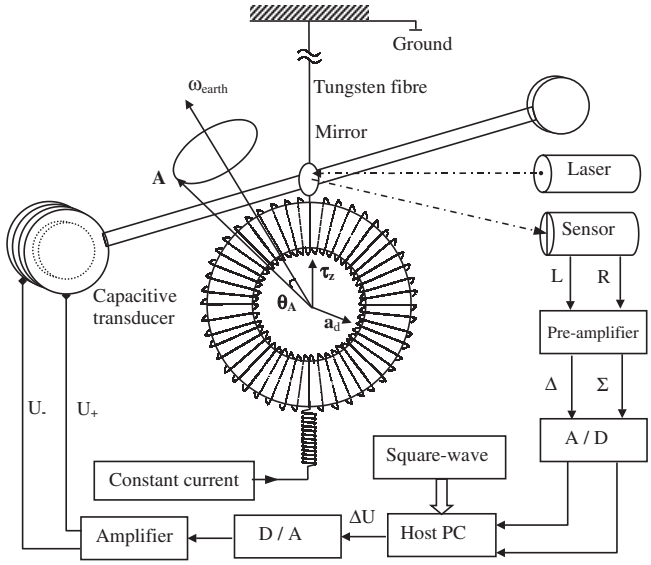


Figure 9. The experimental setup of the rotating torsion balance of Luo *et al* (2003). A steel toroid, having an inner diameter of 45.0 mm, with a cross section 24.0 mm in diameter, was suspended by a tungsten fibre 100 μm in diameter and 136.4 cm in length to form a Cavendish torsion balance. A coil of 1720 turns was wound on the steel toroid, and it carried an electric current of 16.4 mA, which was supplied by a constant-current source through a fine aluminium spring. The magnetic dipole vector-potential moment, a_d arising from the toroidal coil interacted with the cosmic vector potential, A, to produce a torque on the torsion balance, the motion of which was detected by an optic lever, with the data then collected continuously by a host computer. Any external torque was compensated by a capacitive transducer such that the torsion balance was always maintained in its initial equilibrium state through the parallel capacitor plates. The whole system was mounted in a vacuum chamber and held at 1×10^{-2} Pa and was rotated with a period of 1 h by means of a precise rotary table (not shown in this figure). If the photon mass were nonzero, the feedback voltage applied on the capacitive transducer, associated with the effect of photon mass, would vary with time, following the rotation of the torsion balance.

equation (4.30)), which was usually higher than the Earth's rotational frequency Ω. In this case, the torque acting on the torsion balance can be written as

$$\tau_z(\omega) = \mu_\gamma^2 A a_d C \cos(\omega t + \theta_0), \tag{4.31}$$

where

$$C^2 = (\cos\theta_A \cos\lambda - \sin\theta_A \sin\Omega t \sin\lambda)^2 + (\sin\theta_A \cos\Omega t)^2. \tag{4.32}$$

The parameter C in (4.31) is clearly time dependent and hence τ_Z will have a time-varying amplitude. If $\theta_A = 90^\circ$, then the frequency of τ_Z, the signal to be determined, will contain sum and difference terms of the turntable and the sidereal rotation frequencies. In the most general case ($\theta_A \neq 90^\circ$), τ_Z will have a constant component at the turntable frequency in addition to the variable components at the other frequencies mentioned above. This means that at least three peaks will be seen in the power spectrum produced by a fast Fourier transform (FFT) of the experimental data. To estimate the magnitude of C, they averaged it over a sidereal period (24 h) and found its root-mean-square (RMS) value to be

$$\bar{C} = \sqrt{\langle C^2 \rangle} = \sqrt{\frac{3}{4} - \frac{1}{8}\sin^2\theta_A} \geqslant \frac{\sqrt{10}}{4}. \tag{4.33}$$

中国科技论文在线 http://www.paper.edu.cn

A nonzero $\bar{C}$ means that the modulation method can ensure effective detection for all possible orientations of the ambient cosmic vector potential during a sidereal day. Moreover, the limitation from $1/f$ noise will be reduced and the sidereal noises due to environmental fluctuations will be essentially eliminated because of the high modulation frequency. Their analysis of the experimental data (72 h) showed that the product of photon mass squared and the ambient vector potential was $\mu_\gamma^2 A < 1.1 \times 10^{-11}\,\mathrm{Tm\,m^{-2}}$. If the ambient cosmic vector potential is 10^{12} Tm, corresponding to the Coma galactic cluster (0.2 μG over a distance of 4×10^{22} m) (Rand and Kulkarni 1989, Zwiebel 1991), then the upper limit on the photon mass would be 1.2×10^{-51} g. However, the cosmic vector potential can be conservatively estimated from the galactic magnetic field ($\approx$1 μG) and its reversal position ($\approx 1.9 \times 10^{19}$ m) towards the centre of the Milky Way (Asseo and Sol 1987). In that case, $A \approx 2 \times 10^9$ Tm and the corresponding upper limit on the photon mass becomes 2.6×10^{-50} g.

After the result of the rotating torsion balance experiment was published, Goldhaber and Nieto (2003) commented on a potential problem with the use of this approach to setting limits on the photon rest mass. They pointed out that the typical value of the ambient magnetic vector potential $\boldsymbol{A}$ could vanish, or at least be much smaller, in a particular measurement region, and if we happened to be in such a vacant zone, the magnitude of $\boldsymbol{A}$ at our location might not lead to a useful constraint on m_γ. They further noted that the plasma current method (discussed in section 5.4) could overcome this problem. The main difference between the torsion balance and plasma current methods is the region involved: the former interrogates a relatively small local region while the latter surveys on a large astronomical scale. At present, incomplete knowledge of the largest-scale magnetic fields (i.e. at the galactic or even extragalactic level) indeed introduces the possibility of substantial inhomogeneity both in the fields themselves and in the plasma density. Furthermore, uncertainty about the degree of inhomogeneity in the Coma cluster or even in our local galactic cluster makes it hard to quote a typical value for $\boldsymbol{A}$, let alone the systematic uncertainty in it. So, while the results of the torsion balance method indeed gave a value for the local limit on $\mu_\gamma^2 \boldsymbol{A}$, when used to deduce a limit on the photon mass the result is open to question.

4.6. Other approaches

In 1971, Franken and Ampulski proposed a 'table-top' experiment with very low-frequency parallel resonance circuits to set an upper limit on the photon rest mass. They contended that the relationship between the resonance frequency of the LC circuit and the photon rest mass would be governed by

$$\omega'^2 = \omega_0^2 + \omega_c^2, \tag{4.34}$$

where ω_0 is the natural resonance frequency in the zero-mass photon case, which could be calculated theoretically, and $\omega_c = \mu_\gamma c$. From measurements on such a circuit operating at a frequency of $\approx$1 rad s^{-1}, they obtained a result of $m_\gamma < 10^{-49}$ g. However, as pointed out by Goldhaber and Nieto (1971a,b), the crucial problem inherent in this method is that the natural resonant frequency $\omega_0 = (LC)^{-1/2}$ cannot be shifted by more than a fraction of order $(\mu_\gamma D)^2$, where D denotes the dimension of the apparatus. This is because the fields acting on charges and currents in the circuit are only changed by this amount compared with those of the massless photon case. So, the resonance at $\omega = \mu_\gamma c$ would occur for $\omega_0 \approx \mu_\gamma c$, not $\omega_0 = 0$, which means that the photon mass effect in the resonant circuit method is practically negligible. The same conclusion was also reached by Park and Williams (1971), Kroll (1971) and Boulware (1971).

中国科技论文在线 http://www.paper.edu.cn

5. Extra-terrestrial limits on the photon mass

5.1. General introduction

It is arguably the case that most physicists now believe that the photon rest mass is exactly zero. All of the experiments undertaken to date have led only to ever more stringent limits on it, and it is tempting to think that the experimental possibilities in terrestrial laboratories are close to being exhausted. A trend towards using astrophysical methods to reduce the upper limit on the photon rest mass was begun in the 1960s. The basic idea is to find some possible effects of massive photons in a large scale, which might lead to consequences indistinguishable from Maxwellian electromagnetism for phenomena that occur on those scales. In this section, we will discuss the possible astrophysical and cosmological manifestations of a nonzero photon rest mass. Previous discussions of these topics and reviews in this area have been written by Kobzarev and Okun (1968), Goldhaber and Nieto (1971b), Chibisov (1976), Byrne (1977), Dolgov and Zeldovich (1981), Barrow and Burman (1984), and Zhang (1998), among others.

5.2. Dispersion of starlight

Because of intrinsic measurement uncertainties, laboratory investigations of the frequency-dependent dispersion of light under terrestrial conditions have probably reached the limits of the technique. However, because of the great distances involved, astrophysical measurements held promise of improved accuracy. So, efforts were undertaken to search for traces of dispersion arising from a mass of the photon, in cases where the photons were created in astrophysical events. Equation (3.6) shows that a limit on the photon mass could be obtained by comparing the arrival times of pulses of different frequencies that were emitted from the same origin. De Broglie (1940) suggested that observation of the dispersion of radiation from astronomical objects undergoing rapid fluctuation, such as eclipsing binary stars, a pulsar, a supernova, or a quasar, could provide information on the photon rest mass. Specifically, he suggested that a limit on the photon mass could be determined by using light from a star emerging from behind its dark binary companion. He considered the case $\lambda_2^2 - \lambda_1^2 = 5 \times 10^{-13}\,\mathrm{m}^2$ (for instance, red light of $\lambda_2 \sim 800\,\mathrm{nm}$ and blue light of $\lambda_1 \sim 400\,\mathrm{nm}$), $L = 10^3$ light years, and $\Delta t \leqslant 10^{-3}\,\mathrm{s}$. According to equation (3.6), one can obtain (Kobzarev and Okun 1968)

$$m_\gamma \equiv \frac{\hbar}{c}\mu_\gamma \approx \frac{\hbar}{c}\sqrt{\frac{8\pi^2 c\Delta t}{L(\lambda_2^2 - \lambda_1^2)}} \leqslant 8 \times 10^{-40}\,\mathrm{g}.$$

We note that dispersion effects of this kind can be interpreted not only in terms of a photon mass but also in terms of nonlinear effects of electromagnetic fields or the dispersion of light travelling through interstellar plasma in a magnetic field. In fact, these alternative scenarios present the main obstacle in using the technique to determine the photon rest mass more stringently (Gintsburg 1963).

In Maxwellian electromagnetism, the dispersion equation for an electromagnetic wave of frequency ω travelling through plasma is (Goldhaber and Nieto 1971b)

$$k^2 = \frac{\omega^2}{c^2}\left(1 - \frac{\omega_\mathrm{p}^2}{\omega^2 \pm \omega_\mathrm{B}}\right); \tag{5.1a}$$

with

$$\omega_\mathrm{p}^2 = \frac{4\pi n e^2}{m}, \qquad \omega_\mathrm{B} = \frac{eB}{mc}\cos\alpha, \tag{5.1b}$$

in which n is the electron (mass = m) density, α is the angle between the magnetic field B and the direction of propagation of the wave, and ω_p and ω_B are the characteristic frequencies

中国科技论文在线 http://www.paper.edu.cn

of the plasma and the cyclotron frequency of the electron, respectively. Since the magnetic field B is small in interstellar space, the quantity ω_B can be neglected, and the result is then a dispersion similar to the massive photon effect:

$$v_g = \frac{d\omega}{dk} = c\sqrt{1 - \frac{\omega_p^2}{\omega^2}} \approx c\left(1 - \frac{\omega_p^2}{2\omega^2}\right). \tag{5.2}$$

Comparison of equations (3.4) and (5.2) shows that the dispersion resulting from the plasma electron density would produce the same effect as the photon mass μ_γ, i.e. that the effect of ω_p is the same as that of $\mu_\gamma c$ on the dispersion of the speed of electromagnetic waves. Hence, to establish an improved limit on the photon mass by this method, more careful investigations of the plasma in interstellar space would be needed.

The discovery of pulsars provides a way of determining the photon mass by means of a measurement of dispersion in arrival time of radio signals from the pulsars, as mentioned above. A critical parameter in formulating such an estimate is $\bar{n}_e$, the average density of electrons along the path. An approximate formula for plasma-based dispersion is (Feinberg 1969)

$$\frac{4\pi\bar{n}_e e^2}{m_e} = \omega_p^2 \ll \omega^2. \tag{5.3}$$

Hence, according to equations (5.2) and (5.3), and disregarding higher order terms, one obtains an expression for the dispersion for pulsars with different frequencies:

$$\frac{\Delta v_g}{c} \equiv \frac{v_{g1} - v_{g2}}{c} \approx \frac{2\pi\bar{n}_e e^2}{m_e}\left(\frac{1}{\omega_2^2} - \frac{1}{\omega_1^2}\right). \tag{5.4}$$

One possible source of the variation of speed with frequency would arise from photons with mass m_γ. For this case, and recalling equation (3.4), we have

$$\frac{v_g}{c} = \sqrt{1 - \frac{m_\gamma^2 c^4}{\hbar^2\omega^2}} \approx 1 - \frac{1}{2}\frac{m_\gamma^2 c^4}{\hbar^2\omega^2}. \tag{5.5}$$

It is obvious that the variation with frequency due to a photon mass is greatest at small frequencies, thus making propagation at radio frequencies a much more sensitive test of this effect than propagation at optical frequencies. The dependence on frequency is the same as that obtained for plasma dispersion. So, if the plasma has a particle density that exactly cancels the effect induced by the photon mass, we cannot measure the dispersion unambiguously. In this case, if we could place an independent limit on the density of the interstellar plasma, we could place the same limit on the photon mass. Incorporating the two effects (equations (5.2) and (5.5)), Feinberg was able to write

$$\frac{v_g}{c} \approx 1 - \frac{1}{2}\left(\frac{m_\gamma^2 c^4}{\hbar^2} + \omega_p^2\right)\frac{1}{\omega^2}. \tag{5.6}$$

Since the index of refraction is much greater for radio frequencies than for optical frequencies, Feinberg assumed that a substantial part of the observed dispersion would be due to the photon mass effect, and by equating the photon mass and the plasma frequency with which the radio dispersion has been fitted, he arrived at

$$m_\gamma \leqslant \frac{\hbar\omega_p}{c^2} = \frac{\hbar}{c^2}\sqrt{\frac{4\pi e^2\bar{n}_e}{m_e}} = 6 \times 10^{-44}\sqrt{\bar{n}_e}.$$

Staelin and Reifenstein (1968) observed the dispersion of radio signals from the Crab Nebula pulsar (NP0532), and found (assuming zero mass for the photon) an effective average plasma

中国科技论文在线 http://www.paper.edu.cn

density of $\bar{n}_e \leqslant 0.028$ electron cm^{-3}. Using a number such as this, one can easily set a limit on the photon mass of $m_\gamma \leqslant 10^{-44}$ g.

This approach for setting limits on the photon rest mass is obviously quite dependent on the available values of $\bar{n}_e$ that can be used with the pulsar under study, and unfortunately there is not a great deal of relevant existing data (Fabian and Barcons 1991). However, the model is, nevertheless, quite useful, and to the extent that new independent measurements of $\bar{n}_e$ can be made, it may be possible to confirm the speculation that the intergalactic electron density is very small, thus perhaps leading to a more stringent limit on m_γ.

5.3. Magnetostatic effects

One of the most direct consequences of a nonzero photon rest mass arises from its effect on the characteristics of static magnetic fields. As discussed below these effects differ distinctly from those of Maxwellian electromagnetism on length scales greater than the potential Compton wavelength of the photon.

5.3.1. Schrödinger external field. In 1943, Schrödinger proposed a method for determining the photon rest mass. For the case of electromagnetic fields of a certain strength in empty space, and neglecting gravitation, his 'unitary field theory' (Schrödinger 1943a), which posited interactions between gravitons, mesons and electromagnetic fields, suggested that the Compton wavelength 'be not cosmically large (in which case Proca's equations boil down to Maxwell's) but very roughly speaking of the order of the radius of the earth'. In one of his companion papers (Schrödinger 1943b) he placed an upper limit on the photon rest mass by examining a modified version of Maxwell's equations, and specifically Ampère's law. The term that was added acts like 'vertical currents', and by making a fit of the geological data he arrived at a finite photon rest mass. An additional field of the same order of magnitude was also studied by Bicknell (1977), who extended Schrödinger's expression for a dipole field to all orders of the multipole moments by a complete spherical harmonic analysis of static planetary fields. However, Schrödinger pointed out that the effect he predicted could be produced by 'positive or negative particles revolving around the earth at some distance in the equatorial plane ...'.

In his discussion of geomagnetic surveys in 1895, Schmidt pointed out that the geomagnetic field incorporates three types of magnetic fields: 'dipole fields', 'external fields' and 'non-potential fields' (Schrödinger 1943b). The magnetic dipole field, pointing to the south geomagnetic pole, is produced by a magnetic dipole moment. The 'external field', antiparallel to the dipole moment, is a uniform field over the surface of the earth, the origin of which could not be inside the earth. The last type, the 'non-potential field', is produced by a constant current. Subsequent geomagnetic surveys showed that a substantial part of the geomagnetic field is caused by inner sources, i.e. the geomagnetic dipole, and that the external field and the non-potential field accounted for roughly several per cent of the balance. Schrödinger (1943b) argued that the external field 'is that part which Maxwell's theory is obliged to attribute to external sources', while the non-potential field 'refers to the ostensible fact that closed line integrals of the magnetic force do not vanish, which in Maxwell's theory would indicate vertical electric currents in the atmosphere, much stronger than can be accounted for by atmospheric electricity or cosmic rays'. Based on his unitary field theory, Schrödinger examined at some length the concept of a finite photon rest mass, and pointed out that a finite photon rest mass effect could explain the existence of the 'external field' and the 'non-potential field.' His analysis led to an upper limit on it of 2×10^{-47} g (Bass and Schrödinger 1955).

In order to explain the external field effect using the photon rest mass, let us begin with a review of the principles on which the method is based. Consider a stationary current density $\boldsymbol{J}$

中国科技论文在线 http://www.paper.edu.cn

distributed over a small region V, which would generate a constant magnetic field. The massive wave equation becomes

$$(\nabla^2 - \mu_\gamma^2)\boldsymbol{A} = -\mu_0 \boldsymbol{J}. \tag{5.7}$$

A standard solution to the equation is

$$\boldsymbol{A}(\boldsymbol{r}) = \int \boldsymbol{J}(\boldsymbol{r}')G(\boldsymbol{r} - \boldsymbol{r}')\,\mathrm{d}\boldsymbol{r}', \tag{5.8}$$

where G is the Green function with a form of Yukawa potential:

$$G(\boldsymbol{r} - \boldsymbol{r}') = \frac{\mu_0}{4\pi}\frac{\exp(-\mu_\gamma|\boldsymbol{r} - \boldsymbol{r}'|)}{|\boldsymbol{r} - \boldsymbol{r}'|}. \tag{5.9}$$

Substituting the multipole expansion of the Green's function in an area much larger than the dimension of the area V into equation (5.8), one finds the magnetic dipole potential:

$$\boldsymbol{A}(\boldsymbol{r}) \approx \boldsymbol{A}^{(1)}(\boldsymbol{r}) = \frac{\mu_0}{4\pi}\nabla \times \left(\boldsymbol{m}\frac{\mathrm{e}^{-\mu_\gamma r}}{r}\right) \tag{5.10}$$

in which $\boldsymbol{m}$ is defined as a magnetic dipole moment

$$\boldsymbol{m} = \frac{1}{2}\int_V (\boldsymbol{r}' \times \boldsymbol{J}(\boldsymbol{r}'))\,\mathrm{d}\boldsymbol{r}'. \tag{5.11}$$

Correspondingly, for a magnetostatic field, the field of a dipole is given by

$$\boldsymbol{H} \approx \boldsymbol{H}^{(1)} = \nabla \times \boldsymbol{A}^{(1)} = \frac{\mu_0}{4\pi}\nabla \times \nabla \times \left(\boldsymbol{m}\frac{\mathrm{e}^{-\mu_\gamma r}}{r}\right) \tag{5.12}$$

and hence

$$\boldsymbol{H} \approx \boldsymbol{H}^{(1)} = \frac{\mu_0}{4\pi}\frac{\mathrm{e}^{-\mu_\gamma r}}{r^3}\left\{\left(1 + \mu_\gamma r + \frac{1}{3}\mu_\gamma^2 r^2\right)(3\boldsymbol{m}\cdot\hat{\boldsymbol{r}}\hat{\boldsymbol{r}} - \boldsymbol{m}) - \frac{2}{3}\mu_\gamma^2 r^2 \boldsymbol{m}\right\}. \tag{5.13}$$

If we let the dipole $\boldsymbol{m}$ point in the direction of the z-axis ($\boldsymbol{m} = m\hat{z}$, $\hat{z} \equiv \boldsymbol{z}/z$), the components of $\boldsymbol{H}$ can be decomposed to yield

$$H_z = \frac{\mu_0}{4\pi}\left[\left(-\frac{1}{r^3} + \frac{3z^2}{r^5}\right)m' - \frac{2}{3}\frac{\mu_\gamma^2 m}{r}\mathrm{e}^{-\mu_\gamma r}\right], \qquad H_x = \frac{\mu_0}{4\pi}\frac{3zx}{r^5}m', \tag{5.14}$$

where $m' = (1 + \mu_\gamma r + \frac{1}{3}\mu_\gamma^2 r^2)m$. These indicate that the dipole field includes two parts: an ordinary magnetic dipole field as in Maxwell's theory ($\mu_\gamma = 0$) with the dipole strength of

$$\boldsymbol{H}_\mathrm{D} = \frac{\mu_0}{4\pi}\frac{m'}{r^3}(3\hat{z}\cdot\hat{\boldsymbol{r}}\hat{\boldsymbol{r}} - \hat{z}) \tag{5.15}$$

and a new field in the z-direction

$$H_\mathrm{ext} = -\frac{\mu_0}{4\pi}\frac{2\mu_\gamma^2}{3r}\mathrm{e}^{-\mu_\gamma r}m \tag{5.16}$$

with a negative sign that reinforces the equatorial field and weakens the polar field of the dipole. This new field, uniformly distributed on the surface of the earth, is antiparallel to the direction of the magnetic dipole moment $\boldsymbol{m}$. Schrödinger interpreted this 'homogeneous' field as the 'external field' and used this method to analyse the geomagnetic field from the 1922 magnetic surveys, obtaining the ratio of the 'external field' H_ext to the dipole field H_D at the equator of the earth ($\hat{z}\cdot\hat{\boldsymbol{r}} = 0$) as

$$\frac{H_\mathrm{ext}}{H_\mathrm{D}} = \frac{(2/3)\mu_\gamma^2 R^2}{1 + \mu_\gamma R + (1/3)\mu_\gamma^2 R^2} = \frac{539}{31\,089} \tag{5.17}$$

中国科技论文在线 http://www.paper.edu.cn

which gives

$$\mu_\gamma R = 0.176. \tag{5.18}$$

Substituting the radius of the Earth for R, this yielded a photon rest mass of $m_\gamma \leqslant 1.0\times10^{-47}$ g. Bass and Schrödinger (1955) suggested that multiplying this result by a factor of 2 (for a safety margin) gave a more reliable upper bound: $m_\gamma \leqslant 2.0 \times 10^{-47}$ g.

Goldhaber and Nieto (1968) improved on Schrödinger's results by using Cain's fit to geomagnetic data from earthbound and satellite measurements. They argued that the significance of the limit on the external field depended crucially on the reliability of Cain's fit to the geomagnetic field. To take into account the possibility of systematic errors in Cain's fit and any errors in the estimates of true external fields, they generously magnified the error in their estimate and arrived at an upper limit on the rest mass of the photon of $m_\gamma \leqslant 4 \times 10^{-48}$ g. This result corresponded to a photon Compton wavelength of 81 times the radius of the earth, and was five times better than the result of Schrödinger.

Davis *et al* (1975) applied Schrödinger's external field method to an analysis of the Pioneer-10 data on the magnetic field of Jupiter. During the course of the data processing, the photon rest mass was treated as a free parameter, and the standard least-squares procedure was applied to determine the best-fit coefficients in a spherical-harmonic expansion of the Pioneer-10 observations of Jupiter's magnetic field. By taking full advantage of the larger radius and stronger magnetic field of Jupiter, they finally set an upper limit on the photon mass of $m_\gamma \leqslant 8 \times 10^{-49}$ g, which is the smallest limit so far obtained from direct measurements by using Schrödinger's external field method.

In 1994, Fischbach *et al* derived a new geomagnetic limit on the photon mass from an analysis of the satellite measurements of the Earth's magnetic field. After considering the contributions from several different sources, they found that the largest value that $H_{\rm ext}$ could have (at the 1σ level) was $H_{\rm ext} = 11.8$ nT. Using a value of the dipole field of $H_{\rm D} = 30\,573$ nT as found by Langel and Estes (1985), they then concluded that $H_{\rm ext}/H_{\rm D} = 11.8/30\,573 \leqslant 3.9 \times 10^{-4}$ and that the resulting limit on the photon mass was $m_\gamma \leqslant 1 \times 10^{-48}$ g, a value quite close to that obtained from the analysis of Jovian data.

The Schrödinger external field method has provided the most convincing limits on the photon rest mass as derived from astronomical magnetic surveys, and the results from it are compatible with other aspects of the present knowledge in this area. However, at larger scales, it is difficult to separate planetary magnetic fields from those produced by currents flowing in the surrounding plasma. Therefore, the significance of limits placed on the photon mass by this approach depends crucially on the reliability of the method of data analysis. When extracting the external field from satellite measurements of geomagnetic fields or those of Jupiter, a variety of plausible sources of systematic effects require very careful study. These include the solar wind, the density of the surrounding plasma, the satellite trajectory, etc. Hence, several different approaches are conventionally used to verify the validity of the model-dependent data analysis.

5.3.2. Altitude-dependence of massive photon geomagnetic fields. In Maxwell's theory, the strength of the geomagnetic field decreases via an inversely proportional relation to altitude. However, in massive photon electromagnetism, this relation instead describes the exponential decay of the geomagnetic field as altitude increases. So, using the data measured by satellites at different altitudes, one could determine the photon rest mass by detecting the characteristics of the exponential decay of the geomagnetic field.

中国科技论文在线 http://www.paper.edu.cn

The decay of the geomagnetic field with altitude can be approximated by expanding equation (5.13) in a power series in $\mu_\gamma r$ (Zhang 1998),

$$H^{(1)}(\mu_\gamma r) = H_{\rm D}\left[1 + \frac{(\mu_\gamma r)^2(1-5\cos^2\theta)}{2(1+3\cos^2\theta)} + {\rm O}(\mu_\gamma r)^3\right] \approx G(\mu_\gamma, r, \theta)H_{\rm D} \tag{5.19}$$

in which θ is the angle between the direction of the magnetic dipole moment $\boldsymbol{m}$ and $\hat{\boldsymbol{r}}$, and

$$G(\mu_\gamma, r, \theta) = 1 + \frac{(\mu_\gamma r)^2(1-5\cos^2\theta)}{2(1+3\cos^2\theta)},$$

$$H_{\rm D} = \frac{\mu_0}{4\pi}\frac{1}{r^3}|(3\boldsymbol{m}\cdot\hat{\boldsymbol{r}}\hat{\boldsymbol{r}} - \boldsymbol{m})| = \frac{\mu_0}{4\pi}\frac{m}{r^3}\sqrt{1+3\cos^2\theta}.$$

This method couples the photon rest mass with variation in altitude, and can efficaciously distinguish the effect from others which happen to be height independent. On the other hand, because of certain external perturbations, this method can become ineffective when the altitude exceeds a certain limit, which is roughly three times the radius of the earth for the geomagnetic field.

The first limit obtained by this method was by Gintsburg (1963), who used the geomagnetic field data at varying altitudes from the Vanguard, Explorer and Pioneer satellites and assumed $G(\mu_\gamma, r, \theta) = 1-(\mu_\gamma r)^2$. His limit was $m_\gamma < 3\times10^{-48}$ g. It was amended by Goldhaber and Nieto (1968) who, after a more conservative error estimate, arrived at $m_\gamma < (8\text{–}10)\times10^{-48}$ g.

5.3.3. Eccentric dipole effects due to a massive photon. In fact, the real geomagnetic field is closer to that produced by an eccentric dipole. The location of this eccentric dipole is at 6.5° North latitude and 161.8° East longitude, and the distance between the geocentre and the eccentric dipole origin is 342 km (Schrödinger 1943b). From expression (5.10), the lines of vector potential are circles around the magnetic dipole axis, and hence would intersect the surface of the Earth. This means that the integral of this magnetic field along an arbitrary closed path on the surface of the Earth would be nonzero, which corresponds to an existing imaginary current perpendicular to the Earth's surface. For an eccentric dipole with an eccentricity distance of d, the effect produced by a finite photon rest mass would be $d/R = 342/6378 \approx 1/19$ times smaller than that of the external field method at the surface of the Earth, which indicates that the eccentric dipole effect will not yield a more stringent limit on the photon rest mass than the external field method, even if the imaginary current could be distinguished.

5.4. Magnetohydrodynamic effects

It is well-known that magnetohydrodynamic (MHD) phenomena are characterized by a combination of ordinary hydrodynamics and Maxwellian electromagnetism, which is then used to describe the interactions between magnetic fields and a free fluid. If the photon possesses a finite rest mass, MHD phenomena within the interplanetary plasma (e.g. hydrodynamic wave couplings to the interplanetary magnetic field) might provide useful approaches for determining the size of that mass due to its effect on their ordinary Maxwellian description. A self-consistent set of MHD equations accounting for finite photon mass was developed by Ryutov (1997), whose careful analysis of various astrophysical observations led to interesting approaches for making improvements to estimates of the photon mass. Ryutov used this model to investigate the fields due to the solar wind at various points within the Earth's orbit, and concluded that, 'to reconcile observations to theory, one has to reduce m_γ by approximately an order of magnitude compared with Davis in 1975', i.e. $m_\gamma \leqslant 1\times10^{-49}$ g $\equiv 6\times10^{-17}$ eV. This value is the one that

中国科技论文在线 http://www.paper.edu.cn

is currently recommended by the Particle Data Group in their recent compendium (Eidelman *et al* 2004). In what follows we examine some of the relevant MHD phenomena more closely.

5.4.1. Dispersion of hydromagnetic waves. After the theoretical prediction of hydromagnetic waves by Alfvén (1942, 1950), the existence of such waves was subsequently demonstrated in the laboratory by several workers (Lundquist 1949, Lehnert 1954, Sugiura 1961), and the importance of those waves in geophysics and astrophysics was soon recognized. The medium through which such waves propagate is plasma instead of vacuum. Therefore, after taking a nonzero photon mass into account, we must write a new set of dispersion relations for the two types of hydromagnetic waves. Replacing Maxwell's equations by Proca's equations for this task, we arrive at

$$k^2 = \frac{\omega^2}{V_{\rm A}^2} - \mu_\gamma^2 \qquad \text{for magnetosonic waves} \tag{5.20}$$

and

$$k^2 \cos^2\theta = \frac{\omega^2}{V_{\rm A}^2} - \mu_\gamma^2 \qquad \text{for Alfvén waves,} \tag{5.21}$$

where $V_{\rm A} = \sqrt{H^2/4\pi\rho}$ is the Alfvén velocity, ρ the mass density of plasma and θ the angle between the wave vector $\boldsymbol{k}$ and the external magnetic field $\boldsymbol{H}$. This model suggests that there is a critical frequency $\omega_{\rm c} = \mu_\gamma V_{\rm A}$, such that when $\omega < \omega_{\rm c}$, the waves are attenuated exponentially. Therefore, if we know the critical frequency, we can determine the photon mass through it.

In 1963, Gintsburg proposed that to estimate the upper limit on the photon mass, one might experimentally observe long-period hydromagnetic disturbances that are free of damped oscillations in interstellar space. Meanwhile, in order to determine how the nature of those waves depends on the magnetic field variation, their amplitude should be observed simultaneously at the earth's surface and at several different points in space around the earth. Patel and Cahill (1964) obtained the records of observations of such waves propagating simultaneously in the magnetosphere and on the ground, in the form of magnetograms measured by the Explorer XII Satellite. They found that hydromagnetic waves with a period of 200 s were generated at 5×10^4 km from the centre of the earth, and that those waves travelled to the earth's surface in about 90 s with an amplitude attenuation of $\frac{1}{3}$. By assuming a plasma density $n = 50\,{\rm cm}^{-3}$, and taking the magnetic field to be 100 nT (10^{-3} G), Patel (1965) found the photon mass to be $m_\gamma < 4 \times 10^{-47}$ g, approximately the same value as that of Gintsburg (1963). However, the effect on the calculations due to uncertainties in the particle density and the critical frequency may make these limits at least one or two orders of magnitude less stringent.

By using new observations of the Alfvén waves in the interplanetary plasma detected by spacecraft at one astronomical unit (1 AU $= 1.49 \times 10^{11}$ m, the Earth–Sun distance), Hollweg (1974) was able to search for time varying phenomena based on correlations between the magnetic field and the plasma velocity. He concluded that those waves were of extremely low frequency with a period of less than 1 day in the spacecraft frame of reference. To get the frequency in the local rest frame of the plasma, he asserted that the direction of propagation of the waves should be independent of the wave period. Hollweg considered two extreme cases. First, assuming that the absence of waves with periods longer than 1 day was not due to the presence of the photon mass in equation (5.21), he obtained a stronger but less certain limit of $m_\gamma < 1.1 \times 10^{-49}$ g (corresponding to $V_{\rm A} = 20\,{\rm km\,s}^{-1}$ and $\omega_{\rm c} = 6.3 \times 10^{-6}\,{\rm s}^{-1}$). Then, assuming that the absence of waves with periods longer than 1 day was indeed due

中国科技论文在线 http://www.paper.edu.cn

to a finite photon mass in equation (5.21), he obtained the relatively reliable upper limit of $m_\gamma \leqslant 1.3 \times 10^{-48}$ g (corresponding to $V_A = 20\,\mathrm{km\,s^{-1}}$ and $\omega_c = 7.2 \times 10^{-5}\,\mathrm{s^{-1}}$).

Another upper limit on the photon mass was found by Barnes and Scargle (1975) through observations of hydromagnetic waves in the Crab Nebula. Studies of the central region of the Crab Nebula (Scargle 1969) had indicated that the plasma consisted of an ultra-relativistic electron component and a tenuous lower-energy background component, embedded in a magnetic field that was relatively uniform on the scale $\sim 10^{16}$ m. Quasi-periodic disturbances ($\omega \sim 10^{-6}\,\mathrm{s^{-1}}$) generated in the vicinity of the pulsar propagated across the magnetic field out into the nebula. This series of 'wisps' has been identified as a sequence of magnetoacoustic waves in which the wave compressions produced local enhancements of synchrotron radiation. From the kinetic theory of small-amplitude hydromagnetic waves in relativistic plasma, Barnes and Scargle obtained the dispersion relation for magnetoacoustic waves propagating transversely to the background magnetic field

$$\left(\frac{\omega}{kc}\right)^2 \left[1 + \frac{4\pi}{B^2}(\varepsilon + P_\perp)\right] = 1 + \frac{2\pi P_\perp}{B^2}(4 - \zeta) + \frac{\mu_\gamma^2}{k^2}, \tag{5.22}$$

where $P_\perp$ is the total plasma pressure transverse to the background magnetic field B, ε the total energy density (including rest mass), and ζ a numerical factor between 0 and 1. Equation (5.22) implies that the critical frequency of waves propagating ($k^2 > 0$) in the nebula will be

$$\omega_c = \mu_\gamma c \left(1 + \frac{4\pi}{B^2}(\varepsilon + P_\perp)\right)^{-1/2}. \tag{5.23}$$

Barnes and Scargle (1975) estimated the magnitude of the parameters from analysis of photographic measurements of the Crab Nebula (Scargle 1969) and argued that the uncertainties in those parameters arose mostly from ambiguities in interpretation, due to inadequate determination of the time histories of the rapidly moving features, rather than from more standard measurement uncertainties. They arrived at a final upper bound on the photon mass of $m_\gamma \leqslant 3 \times 10^{-54} \sim 3 \times 10^{-53}$ g, which represented an improvement of four to five orders of magnitude over the other contemporary limits on the photon mass at that time.

However, Barnes and Scargle (1975) pointed out that although the standard arguments (Gintsburg 1963, Patel 1965, Goldhaber and Nieto 1971b) for inferring upper limits on the photon rest mass from cosmic hydromagnetic waves gave plausible but not rigorous limits, they derived from an essential yet intrinsic assumption that the background plasma is infinite and uniform. Moreover, one simple consequence of the Proca equations is that either a static magnetic field varies perceptibly over the scale of order μ_γ^{-1}, or there is a large background current $\boldsymbol{J}_0 \approx \mu_0^{-1}\mu_\gamma^2 \boldsymbol{A} (J_0 \gg \mu_0^{-1}|\nabla \times \boldsymbol{B}|)$. In either case, the dispersion relation breaks down for $k \leqslant \mu_\gamma$. Consequently, the upper limits of the photon rest mass obtained by this method would then be open to doubt. Byrne (1977) has pointed out that for a correct treatment, the dispersion relation would need to be derived self-consistently from the Proca equations and the plasma equations. Until that is done, the limits mentioned in this subsection may not be completely free of interpretation.

5.4.2. Dissipation of the interplanetary magnetic fields. Hydromagnetic theory says that a conducting medium moving in a magnetic field would generate an induced electromotive force. Generally, the finite conductivity of the medium would cause an exponential attenuation of the magnetic field, the rate of which is determined by the size of its conductivity and the dimensions of the supporting plasma. However, when considering the additional effects of a finite photon rest mass, the situation would be different.

中国科技论文在线 http://www.paper.edu.cn

Williams and Park (1971) considered this case and pointed out that the field would diminish at a rate determined by the plasma dimensions and the photon's Compton wavelength, the smaller number predominating. They assumed a galactic arm that had been straightened out so as to form a long filament of plasma with a magnetic field running down it, and supposed that the plasma is electrically neutral and that there is no electric field along the filament, so that the currents flow perpendicular to its length. Moreover, they assumed that the spatial distribution of the galactic plasma does not change dramatically for periods of the order of 10^6 years. After making these assumptions, there was no need to deal directly with the hydrodynamic equations for the plasma, but rather only with the damping force and the electromagnetic force acting on the electrons and ions. By use of the Proca equations, and ignoring inertial forces, they found that the dissipation of the magnetic energy in the arm of the galaxy was

$$W \sim \exp\left[-\frac{2\nu}{l^2}(1+\mu_\gamma^2 l^2)t\right], \tag{5.24}$$

where $\nu = c^2/4\pi\sigma_\mathrm{i} \approx 10^{23}\,\mathrm{cm^2\,s^{-1}}$ with $\sigma_\mathrm{i} \approx 10^{-3}\,\mathrm{s^{-1}}$ as per the known properties of cool plasma in the HI zones of the galaxy, and l is the length of the order of the radius of the spiral arm. The dissipation time of this magnetic energy would thus be

$$\tau \sim \frac{l^2}{2\nu}(1+\mu_\gamma^2 l^2)^{-1}. \tag{5.25}$$

The flux of primary cosmic rays has remained roughly constant on average over the last million years, which indicates that $\tau \sim 10^6$ years. By assuming that the field has remained unchanged over this time span and by further accepting all of the astrophysical hypotheses mentioned earlier, Williams and Park gave an upper bound to the photon rest mass of $m_\gamma < 3.4\times10^{-56}$ g.

Byrne and Burman (1972) re-examined the dissipation of large-scale magnetic fields in the Galaxy and pointed out that Williams and Park (1971) had adopted a common misinterpretation of the tensor conductivity. Considering a three-fluid plasma consisting of electrons, protons and identical neutral particles, and ignoring the inertial force and pressure gradients, Byrne and Burman claimed that, when the conductivity is effectively infinite, the magnetic flux is 'frozen-in' to closed contours moving with the velocity of the magnetic field, which is much closer to the electron velocity than to the bulk velocity of the combined electron–proton fluid. The conductivity relevant to both Joule heating and the rate of diffusion of lines of the magnetic field is defined by

$$\sigma^{-1} = \frac{m_\mathrm{e}}{ne^2}\left[\nu_\mathrm{ei} + \left(\frac{m_\mathrm{i}}{m_\mathrm{i}+m_\mathrm{e}}\right)^2 \nu_\mathrm{en} + \frac{m_\mathrm{i}m_\mathrm{e}}{(m_\mathrm{i}+m_\mathrm{e})^2}\nu_\mathrm{in}\right], \tag{5.26}$$

where n is the electron or proton number density, e the charge on a proton, and m is the particle mass with subscripts e, i and n denoting quantities pertaining to the electron, proton and neutral particle fluids, respectively. The momentum relaxation frequency ν_ab represents the rate of collisions of particles of the component fluid a with particles of the component fluid b in the above expression. In interstellar space, the electron–proton collision frequency is much larger than the electron–neutral and proton–neutral collision frequencies, and hence the friction between the combined electron–proton fluid and the neutral fluid can be neglected. Using Faraday's law and the Proca equation, and ignoring the displacement current and gradients of the conductivity, Byrne and Burman obtained

$$\frac{\partial \boldsymbol{H}}{\partial t} = \nabla\times(\boldsymbol{u}_\mathrm{H}\times\boldsymbol{H}) + \frac{c^2}{4\pi\sigma}(\nabla^2\boldsymbol{H} - \mu_\gamma^2\boldsymbol{H}), \tag{5.27}$$

where $\boldsymbol{u}_\mathrm{H}$ could be referred to as the velocity of the magnetic field. The first term in equation (5.27) is the same as that in usual hydromagnetics, in which the magnetic field is

中国科技论文在线 http://www.paper.edu.cn

'frozen' into the medium. The last two terms denote the dissipation effects of the interstellar magnetic field. Using L to denote the distance over which the magnetic field $\boldsymbol{H}$ varies significantly, $\nabla^2\boldsymbol{H} \sim L^{-2}H$. The dispersion in equation (5.27) implies that the magnetic field $\boldsymbol{H}$ decays as $\exp(-t/\tau)$ with

$$\tau \approx 2\pi\sigma c^{-2}(L^{-2} + \mu_\gamma^2)^{-1}. \tag{5.28}$$

For the region $L \gg \mu_\gamma^{-1}$,

$$\mu_\gamma \approx \sqrt{\frac{2\pi\sigma}{c^2\tau}}. \tag{5.29}$$

In interstellar space, $\sigma \approx ne^2/m_e v_{ei}$, and $v_{ei} \approx 5.5n\ln(220Tn^{-1/3})T^{-3/2}$ (Ginzburg 1970) with T denoting the temperature, and thus

$$\sigma \approx \frac{e^2}{m_e}\frac{T^{3/2}}{5.5\ln(220Tn^{-1/3})}. \tag{5.30}$$

Hence, the conductivity σ depends strongly on T but only slightly on n. According to equations (5.30) and (5.31), the variation of μ_γ with T is more significant than that with τ, and so the best upper limit for photon mass that comes from considering the dissipation of large-scale magnetic fields will be for the case where one is investigating a cool region with long-lived fields.

Applying those expressions to galactic HI regions, and using $T \leqslant 10^2\,\mathrm{K}$ and $n \approx 10^{-3}$–$10^{-2}\,\mathrm{cm}^{-3}$ yields $\sigma \leqslant 5 \times 10^9\,\mathrm{s}^{-1}$. If the existence of large-scale magnetic fields in HI regions with $\tau \geqslant 10^6$ year is established, a reduced limit of $m_\gamma < 4 \times 10^{-50}\,\mathrm{g}$ is found. On the other hand, if there is a general galactic magnetic field, the dissipation time τ can be estimated to be at least equal to the rotation period of the galaxy, i.e. 2×10^8 year. Furthermore, if the temperature T is assumed to remain approximately the same over that time, then the corresponding limit on the photon mass would be $m_\gamma < 4 \times 10^{-51}\,\mathrm{g}$, and the Compton wavelength for it reaches 1 AU. If there exists a medium with $T \sim 10^4\,\mathrm{K}$ with cool HI regions embedded in it, then $m_\gamma < 10^{-49}\,\mathrm{g}$. From the information that was known at the time about the interstellar medium (ISM) and field, a conservative upper limit for the photon mass was obtained by considering magnetic fields with a scale of a few hundred parsecs, $T \leqslant 10^4\,\mathrm{K}$ and $\tau \geqslant 10^6$ year. The result was $m_\gamma < 10^{-48}\,\mathrm{g}$, which represented a modest improvement over the upper limit that had been established by (Goldhaber and Nieto 1971b) of $m_\gamma < 4 \times 10^{-47}\,\mathrm{g}$.

5.4.3. Stability of current density in the ISM. If the photon possessed a finite rest mass, then Proca's equations could be used to deduce the charge and current densities underlying electric and magnetic fields. Moreover, if the dimensions of the fields are greater than the reduced Compton wavelength of the photon, then the structures of the fields as derived from Proca's equations would be significantly different from those derived from Maxwell's equations. In their review of theoretical and experimental work on the photon rest mass, Goldhaber and Nieto (1971b) proposed another astrophysical method: one can use the conditions for the existence and stability of the current densities needed to produce the observed galactic magnetic field to place an upper limit on the photon rest mass from a knowledge of the size of that field.

Following Goldhaber and Nieto, Byrne and Burman (1973) then developed this method in detail. It has been shown (Alfvén and Carlqvist 1967, Alfvén 1968, Carlqvist 1969) that a plasma becomes unstable and locally evacuated, with a corresponding large fall in conductivity, when the electron drift velocity V exceeds the electron thermal speed U_e. Also, when V exceeds the phase speeds of some types of waves, instabilities can occur. For example, the magnetosonic over-stability arises when V exceeds the Alfvén speed V_A. If V_m denotes the

中国科技论文在线 http://www.paper.edu.cn

maximum electron drift speed that the plasma can support stably, then the maximum current density that could exist in the plasma is $j_{\rm m} = neV_{\rm m}$, in which n is the electron number density and e the electronic charge. Obviously, the maximum current density that can exist in interstellar space would be $j_{\rm m} \sim nec$ when the maximum electron drift speed is equal to the speed of light.

Let L_1 represent the characteristic length over which the vector potential field $\boldsymbol{A}$ varies significantly; then $|\nabla^2 \boldsymbol{A}| \sim L_1^{-2} A$. According to Proca's equations, if $L_1 \gg \mu_\gamma^{-1}$, the equation for $\boldsymbol{A}$ becomes

$$\mu_\gamma^2 \leqslant \frac{\mu_0 j_{\rm m}}{A}. \tag{5.31}$$

The vector potential field is not directly observable, and there is insufficient information about the geometry of the magnetic field of the galaxy to deduce $\boldsymbol{A}$. Nor can the current density of interstellar space be directly measured. However, an approximation for the strength of the vector potential field can be made by taking $A \approx HL_2$ with L_2 denoting another characteristic length over which the vector potential field $\boldsymbol{A}$ varies significantly. For the MHD situation, both L_1 and L_2 will usually be the smallest dimension of a quasi-uniform magnetic field. Thus, expression (5.31) reduces to

$$\mu_\gamma^2 \leqslant \frac{\mu_0 neV_{\rm m}}{H \min(L_1, L_2)}. \tag{5.32}$$

Making use of the data, $H \sim 10^{-6}\,{\rm G}$, $V_{\rm m} \leqslant 10^3\,{\rm m\,s^{-1}}$, $n \leqslant 1\,{\rm cm^{-3}}$ and $L \approx 10^{19}\,{\rm m}$, Goldhaber and Nieto (1971b) obtained a limit of $m_\gamma < 4\times10^{-53}\,{\rm g}$. Through a consideration of various instabilities in the ISM of the galactic HI regions, Byrne and Burman (1973) established a limit on the photon rest mass of $m_\gamma < 10^{-52}\,{\rm g}$ for the case where the intercloud medium is hot ($\approx 10^4\,{\rm K}$), and $m_\gamma < 4 \times 10^{-53}\,{\rm g}$ when the HI clouds are cool ($<10^2\,{\rm K}$). More recently, Goldhaber and Nieto (2003) arrived at a limit of $m_\gamma < 10^{-52}\,{\rm g}$ for dimensions on the scale of the Coma cluster (Asseo and Sol 1987, Kronberg 1994, 2002) using the same method.

On the other hand, the maximum current density in the ISM can be obtained from a consideration of the heat balance in the medium. One can calculate the rate Λ at which thermal energy is lost by all processes (Byrne and Burman 1973, Burman and Byrne 1973, Byrne 1977) and, in thermal equilibrium, the rate of Joule heating, j^2/σ, cannot exceed Λ. Hence $j_{\rm m}^2 \leqslant \sigma\Lambda$, and from equations (5.31) and (5.32),

$$\mu_\gamma^2 \leqslant \frac{\mu_0\sqrt{\sigma\Lambda}}{H \min(L_1, L_2)}. \tag{5.33}$$

Byrne and Burman (1973) discussed the values of σ and Λ in the ISM and showed that the current density $\sqrt{\sigma\Lambda}$ is about five orders of magnitude less than the maximum value $j_{\rm m} \sim nec$ that the medium can support. Hence, an upper limit of $m_\gamma < 4 \times 10^{-53}\,{\rm g}$ is obtained, which is similar to the value found from stability considerations. An alternative interpretation of this result is that if the photon rest mass is $m_\gamma \sim 4 \times 10^{-53}\,{\rm g}$, then a major heating mechanism of the ISM is Joule heating due to the passage of a current. In fact, there is sufficient energy in the magnetic field of the galaxy to support heating at this rate. Byrne and Burman (1975) analysed this case.

For a magnetic field of dimensions greater than the reduced Compton wavelength of the photon, the dominant contribution in the energy density of the massive photon electromagnetic field (see equation (2.17)) is $\mu_\gamma^2 \boldsymbol{A}^2/2\mu_0$, which is of the order of $\mu_\gamma^2 H^2 L^2/2\mu_0$, where L is the size of the smallest dimension for an approximately uniform magnetic field. If ρ denotes an upper limit on the mean mass density of matter and energy in all forms that could exist

中国科技论文在线 http://www.paper.edu.cn

in a region of space in which a magnetic field is observed, then $\mu_\gamma^2 \boldsymbol{A}^2/2\mu_0 c^2 \leqslant \rho$, and hence

$$\mu_\gamma^2 \leqslant \frac{2\mu_0 c^2 \rho}{H^2 L^2}. \tag{5.34}$$

The galactic magnetic field in the vicinity of the Sun has been observed (Manchester 1974) to have a strength of $\approx$0.2 nT (2×10^{-6} G) and is approximately uniform over a distance of at least 300 parsecs (1 parsec $= 3.08 \times 10^{16}$ m). The masses of galaxies may be estimated from their rates of differential rotation and from the orbital velocities of binary star systems in them; a conservative upper limit for the galactic disc is $\rho \leqslant 10^{-21}\,\mathrm{g\,cm^{-3}}$. Assuming that the interstellar magnetic field in the vicinity of the Sun is typical of magnetic fields in the galactic disc, inequality (5.34) leads to $m_\gamma < 10^{-51}$ g. Their explanation of these results is that if $m_\gamma \sim 10^{-52}$ g, the main contribution to the mass of the galactic disc is then due to the energy density $\mu_\gamma^2 \boldsymbol{A}^2/2\mu_0$ associated with the observed galactic magnetic field, the magnitude of which exceeds the Maxwellian energy density by 11 or more orders. On the other hand, it is worth noting that the large energy densities associated with large-scale magnetic fields and a finite photon rest mass could be significant in some astrophysical processes.

However, Chibisov (1976) pointed out that in the method of Byrne and Burman (1975), an important circumstance that could radically alter the conclusions had not been taken into account. Chibisov argued that if one calculated the energy–momentum tensor in macroscopic (distances of the order of the solar diameter) electrodynamics with a nonzero photon mass, the total magnetic pressure P_M is found to consist of the pressure $P_\mathrm{B} = B^2/2\mu_0$ due to the field $\boldsymbol{B}$ and an additional pressure $P_\mathrm{A} = \mu_\gamma^2 A^2/2\mu_0$ due to the vector potential $\boldsymbol{A}$. If the magnetic field $\boldsymbol{B}$ varies over a characteristic length L, then the definition $\boldsymbol{B} = \nabla \times \boldsymbol{A}$ gives $A \sim BL$. The comparison of the magnetic pressure and the pressure of the vector potential shows that the effect of electrodynamics with finite photon mass over a scale L is greater than that over a scale of the photon Compton wavelength. Thus, the photon Compton wavelength is a kind of fundamental length in electrodynamics because Maxwell's equations must be replaced by the Proca equations for scales greater than this fundamental length. This is unusual in that it determines the region of applicability for the theory at large scales, but not at small ones. Chibisov further argued that it is necessary to use the equations of general relativity to calculate correctly the gravitational field of relativistic mass–energy such as the electromagnetic field, in which case those two contributions cancel each other and the galactic magnetic field cannot produce anomalously strong gravitational fields. His re-calculation showed that the mass of the galaxy, as determined from the differential rotation rates, cannot contain a contribution from effects associated with a nonzero photon rest mass, and, therefore, the principal argument of Byrne and Burman (1975) should be superceded. From an analysis of the mechanical stability of the magnetized gas in galaxies, with allowance for the specific pressure forces of the vector potential, Chibisov obtained an upper limit on the photon rest mass of $m_\gamma \leqslant 3 \times 10^{-60}$ g.

As the most stringent bound on the photon mass, Chibisov's method depends in a critical way on assumptions, such as applicability of the virial theorem (Binney and Tremaine 1987), which states that, for a stable, self-gravitating, spherical distribution of equal mass objects (stars, galaxies, etc), the total kinetic energy of the objects is equal to $-\frac{1}{2}$ times the total gravitational potential energy. The virial theorem is a remarkably useful simplifying result for otherwise very complex physical systems such as solar systems or galaxies, and is also applicable to a number of other similar scenarios. However, the structure of the galactic magnetic field is not very well-known and the reliability of this approach thus remains somewhat unclear.

中国科技论文在线 http://www.paper.edu.cn

5.4.4. Other methods. Yamaguchi (1959) argued that there is hydromagnetic turbulence in the large scale motions of interstellar media, particular in the Crab nebula. His idea was that the photon Compton wavelength should not be smaller than the dimension D of such magnetic turbulences. Using the scale of the Crab nebula $D \sim 10^{15}$ m, he obtained an upper limit on the photon mass of $m_\gamma \leqslant 4 \times 10^{-55}$ g. When the same technique was applied to the field in one of the spiral arms of the Milky Way galaxy, Yamaguchi claimed that a limit of $m_\gamma \leqslant 4 \times 10^{-59}$ g could be obtained (Goldhaber and Nieto 1971b).

5.5. Gravitational deflection of massive photons

In 1973, Lowenthal proposed a method for setting limits on the photon mass by exploiting the gravitational deflection of electromagnetic radiation. As is well-known, the theory of general relativity predicts a deflection of starlight by the Sun of 1.75 arcsec (Hawking 1979). If the photon has a nonzero rest mass, this deflection angle would become

$$\theta = \theta_0 \left(1 + \frac{m_\gamma^2 c^4}{2h^2 v^2} \right), \tag{5.35}$$

where $\theta_0 = 4MG/Rc^2$ is the deflection angle for a massless photon, M is the solar mass, G the Newtonian gravitational constant, R the photon impact parameter (normally the solar radius), and hv the photon energy. Lowenthal set the correction term $\Delta = \theta_0(m_\gamma^2 c^4)/(2h^2 v^2)$ equal to the difference between the measured deflection angle and the deflection angle calculated for photons with zero rest mass. By so doing, an expression setting an upper limit on the photon mass could be written as

$$m_\gamma^2 \leqslant \frac{hv}{c^2} \sqrt{\frac{2\Delta}{\theta_0}}. \tag{5.36}$$

Using the above equation and the data available at the time on the deflection of electromagnetic radiation by the Sun, Lowenthal considered three cases and obtained: (1) for visible light, $m_\gamma < 1 \times 10^{-33}$ g with $v = 5 \times 10^{15}$ Hz and $\Delta \approx 0.1$ arcsec; (2) for radio source 3C 270, $m_\gamma < 7 \times 10^{-40}$ g with $v = 3 \times 10^9$ Hz and $\Delta \approx 0.1$ arcsec; (3) for intercontinental baseline interferometry, a promising limit would be $m_\gamma < 7 \times 10^{-41}$ g if the deflection measurement at radio frequencies could be improved to 0.001 arcsec. Recently, Accioly and Paszko (2004) analysed the energy-dependent deflection of a massive photon by an external gravitational field and arrived at the same expressions for setting limits on the photon mass as found in equation (5.36). Using the best measurement of the deflection of radio waves by the gravitational field of the Sun ($\approx 1.4 \times 10^{-4}$ arcsec) and the lowest frequency employed by radio astronomers (≈ 2 GHz), they found a limit of $m_\gamma < 10^{-40}$ g.

The values of m_γ derived from gravitational deflection are considerably weaker than the other bounds obtained recently, and this method for setting limits on the photon mass is, in principle, less precise than the approaches that directly measure the dispersion of light passing through interstellar space (Lowenthal 1973). Even so, the method is an interesting independent approach and its presentation adds to the evidence restricting the size of the photon mass.

5.6. Present difficulties

As seen above, the various limits obtained by what we termed extra-terrestrial methods are several orders of magnitude more stringent than those obtained by terrestrial approaches (see table 3). However, there are a number of inherent difficulties in any approach aimed at making accurate estimates of the photon rest mass. Some of the resulting limits on it are lower than the

中国科技论文在线 http://www.paper.edu.cn

Table 3. Summary of upper limits on the photon mass as obtained by extra-terrestrial methods (in temporal order).

Author (year)	Physical phenomena investigated	Bounds on m_γ g
De Broglie (1940)	Dispersion of starlight (binary stars)	8×10^{-40}
Bass and Schrödinger (1955)	External fields (geomagnetic fields)	2×10^{-47}
Yamaguchi (1959)	Scale of hydro-magnetic turbulences in Crab Nebula	4×10^{-55}
Gintsburg (1963)	Altitude-dependence of massive photon geomagnetic fields	3×10^{-48}
Patel (1965)	Dispersion of hydromagnetic waves (in Earth's magnetosphere)	4×10^{-47}
Goldhaber and Nieto (1968)	External fields (geomagnetic fields)	4×10^{-48}
	Altitude-dependence of massive photon geomagnetic fields	$(8–10) \times 10^{-48}$
Feinberg (1969)	Dispersion of starlight (NP0532)	10^{-44}
Williams and Park (1971)	Dissipation of large-scale magnetic fields in Galaxy	3.4×10^{-56}
Goldhaber and Nieto (1971)	Stability of plasma in Galaxy	4×10^{-53}
Byrne and Burman (1972)	Re-examination of Williams and Park's results	4×10^{-50}
Byrne and Burman (1973)	Stability of plasma in Galaxy (for hot intercloud medium)	10^{-52}
	Stability of plasma in Galaxy (for cool intercloud medium)	4×10^{-53}
Lowenthal (1973)	Gravitational defection for radio source 3C 270	7×10^{-40}
Hollweg (1974)	Dispersion of hydromagnetic waves (in interplanetary medium)	1.3×10^{-48}
Davis *et al* (1975)	External fields (Jovian magnetic fields)	8×10^{-49}
Byrne and Burman (1975)	Mean mass density of the galactic disc	10^{-51}
Barnes and Scargle (1975)	Dispersion of hydromagnetic waves (in Crab Nebula)	3×10^{-54}–3×10^{-53}
Chibisov (1976)	Analysis of the mechanical stability of the magnetized gas	3×10^{-60}
de Bernardis *et al* (1984)	Investigation on the spectral behaviour of the cosmic background dipole anisotropy	$(2.9 \pm 0.1) \times 10^{-51}$
Fischbach *et al* (1994)	External fields (geomagnetic fields)	1×10^{-48}
Ryutov (1997)	Analysis of the solar-wind magnetic fields	10^{-49}
Goldhaber and Nieto (2003)	Stability of plasma in Coma cluster	10^{-52}
Accioly and Paszko (2004)	Gravitational defection of radio waves	10^{-40}

recently recommended limit published by the Particle Data Group (Eidelman *et al* 2004); this accepted value is the one taken to be most fundamentally compatible with present knowledge. In any case, many of the models that have been used rely on some crucial assumptions which are sometimes difficult if not impossible to check, at least at present.

It is important to note that almost all of the methods discussed in this section are essentially order-of-magnitude arguments. Much more information would be needed about the structure of the galactic magnetic field in order to find more accurate values. Some of the required quantities include either improved estimates, inferences or measurements of the vector potential field, the current density, the particle number density, etc. Order-of-magnitude arguments are seldom convincing unless the argument itself is not sensitive to changes of several orders of magnitude in the values of the parameters that are involved. This caveat is met in some of the cases, since the upper limit to be obtained on the photon rest mass in them varies as the square root of those parameters, but this is not so in all the cases. On the other hand, the physical properties of the ISM, such as the mean electron density, temperature and the electron drift velocity, are different for a spiral galaxy compared to that for clusters of galaxies (Fabian and Barcons 1991). Also, at very large scales, comparatively little is known about the intergalactic medium (IGM) at present. So, as an example, when using astrophysical data to place a limit on plasma currents everywhere in a large region, one is hard pressed to make estimates of the

中国科技论文在线 http://www.paper.edu.cn

systematic uncertainties involved. It is this type of incomplete knowledge about the ISM and IGM (Kronberg 1994, 2002) that makes it difficult to use the extra-terrestrial methods to quote precise results for m_γ.

On the other hand, the Proca equations, which are used to develop the fundamental theory for the massive photon, provide the pathway for almost all approaches to detect it. When dealing with m_γ one should distinguish between measurements and estimates performed on large versus small scales, and one should also determine whether Maxwellian or Proca fields are needed to describe the phenomena in the corresponding regions of interest. Unfortunately, it is often difficult to draw these conclusions. As we have seen above, there have been frequent controversies in this field, but this is a healthy sign in scientific research. From the present vantage point, it seems clear that the more approaches that can be developed to gain a comprehensive picture of the microscopic origin of the photon rest mass, the better, since one never knows which specific attempts to improve this limit will *a priori* be the best.

6. Possible future improvements

6.1. Terrestrial experiments

For the dispersion-of-light studies, in order to obtain more stringent bounds on the photon mass one should choose the waves of lower and lower frequencies that propagate over longer and longer distances, both in terrestrial experiments and in extra-terrestrial observations. However, the lower the wave energy, the more difficult the measurement becomes because of dissipation in the medium over the long pathways involved. In practice, the two needs often oppose each other. Due to this inherent restraint, it has been difficult to use this method to improve the limits on the photon rest mass. Füllekrug (2003) proposed that by observing the naturally occurring lightning discharges in the troposphere, which transmit radio waves at extremely-low frequencies (5–50 Hz), the speed of light could be known with an accuracy determined by perturbations of the ionospheric reflection height (≈90–110 km) associated with space weather phenomena. The limit deduced for the photon rest mass by this method is $m_\gamma \leqslant 4 \times 10^{-49}$ g at ∼8 Hz, but there are several points requiring further consideration. For instance, it is difficult to specify the uncertainty of the estimated value, even if this limit is the most generous estimate which one can make by choosing the smallest observed ionospheric reflection height perturbation. These perturbations are associated with the mean solar rotation period, as was shown from 12 years worth of magnetic field measurements that were made starting in 1986. The general technique remains of interest and it occupies a niche similar to other determinations involving fields of the Earth (Fischbach *et al* 1994) and Jupiter (Davis *et al* 1975).

The experiment of Williams *et al* (1971) has placed the best laboratory limit on the photon rest mass to date. However, as discussed above, the sensitivity of laboratory experiments scales as $(\mu_\gamma^2 L)^2$. Hence, one needs to improve the signal-to-noise ratio of such experiments by a factor of 100 to improve the photon mass limit by a factor of 10. Thus, it will be a nontrivial task to go beyond the present laboratory limit. Even so, a significant improvement over the previous experiment appears possible through advances in experimental techniques. There are potentially three ways to improve the experiment (Tu and Luo 2004): (1) choose a larger dimension of experimental apparatus; (2) increase the applied alternating voltage; and (3) detect a smaller potential difference. As for the experimental dimension, the limit on the photon mass goes inversely as the scale of the shells that are used, whether they are simple spheres or have icosahedral geometry. The amplitude of the voltage applied to the outer conducting shell is not limited by theoretical restrictions but rather by practical operation.

中国科技论文在线 http://www.paper.edu.cn

However, the frequency is limited by the approximation used to deduce equation (4.27), namely $kr < 1$ and $\omega > \mu_\gamma c$. Obviously, then, the approximate frequency span over which one can work should be $\mu_\gamma c < \omega < r^{-1}c$, which sets the ultimate limiting frequency at $\approx 10^7$ Hz for a laboratory experiment of acceptable dimensions. The most crucial factor in improving the accuracy of the Cavendish method is to reduce the noise voltage (Johnson 1928, Nyqyist 1928) hence enabling the detection of a smaller potential difference. The various approaches to decreasing the noise are well-known: low temperature operation, long observation times, applying a high frequency ac signal to the concentric shells, and increasing the input resistance. The most promising approach, which would indeed lower the noise voltage by several orders, is to use cryogenic techniques to reduce the temperature of the apparatus to the level of a few millikelvin, in essence following the lead of transforming between room temperature and cryogenic Weber-bar gravitational wave detectors.

As for the torsion balance method, the restrictions on the accuracy of the measurement arise from the thermal noise and related instrumentational limits on the performance of the torsion balance itself, and from the estimation of the cosmic magnetic vector potential. Several of the instrumentational limits are quite well-known and have been discussed by Gillies and Ritter (1993). However, the main difficulty will come from the estimation of the cosmic magnetic vector potential, which clearly depends on obtaining an accurate map of the magnetic field over such large scales of distance, and this is not attainable at present.

6.2. Extra-terrestrial detection

When the Schrödinger external field method is used to determine limits on the photon mass, the pressing need for substantially improved geophysical data make it seem unlikely that a limit lower than that obtained by Fischbach *et al* (1994) can be achieved without them. Among the specific types of data needed are improved measurements of the dimensions of the Earth, its magnetic field strength, and the fields in the solar system in the vicinity of the Earth. It is likely that the best near-term improvements in the technique will come instead from observations of the magnetic fields of Jupiter and of the Sun. By measuring the altitude-dependence of a massive photon geomagnetic field at distances greater than those of the Pioneer 10 survey (Davis *et al* 1975), i.e. from 4 to 100 times the radius of Jupiter as is anticipated for the Galileo probe, a Jovian photon mass limit improved by a factor of 2–4 would be obtained. The most intriguing potential improvement might come from a more accurate set of data on the distribution of the magnetic dipole moment of the Sun inside the range of the solar system, since the Sun has the advantages of larger dimensions and a stronger magnetic field. However, the enormous and varying plasma currents around the Sun would make the magnetic observations quite difficult, as discussed by Ryutov (1997).

As far as MHD effects are concerned, a number of important parameters remain unknown at this point in time. As discussed above, the methods developed via such an approach involve many assumptions, most of which are open to interpretation at present. Even if the limits obtained by MHD effects might possibly be several orders of magnitude lower than those arising from other methods, there are several points in the arguments where such questions arise. Moreover, the MHD effects used to deduce upper limits on the photon rest mass can be interpreted by alternative phenomena. Hence, it is not clear at present that further improvements in the MHD methods will unequivocally lead to tighter actual constraints on m_γ.

6.3. Concluding remarks

We have discussed the past and present upper limits that have been found for the photon rest mass, and we have considered some possible areas where future improvements might occur.

中国科技论文在线 http://www.paper.edu.cn

The concept of establishing a finite mass of the photon is rooted in the field of precision measurement, and the related efforts to make high precision tests of the accuracy of the inverse square law have been traced back to the time of Cavendish. The possibility of arriving at an actual value for m_γ has never been ruled out. Finding a nonzero value for the photon rest mass would have no foreseeable consequences on everyday life and work, and have virtually no impact on the bulk of terrestrial laboratory physics. However, for physics on scales comparable with the Compton wavelength of the photon, the importance would be profound. This is the region of astrophysics and cosmology where many doubts and suspicions await resolution, and determining a nonzero value for the mass of the photon would be of substantial significance for work on the formation and early evolution of stars and stellar systems, the origin and the stability of large scale cosmic magnetic fields, the properties of the interstellar media and plasma, and so on. Hence, it can truly be said that the problem of the photon rest mass is ultimately of interest in both fundamental physics and applied electrodynamics.

The goal of the review has been to introduce the interested reader to the present theoretical and experimental situation regarding the photon mass. While the review is neither fully exhaustive nor completely detailed, we have sought to present a useful cross-section of the literature on the topic and thereby provide a helpful starting point for further study. The interested reader should also consult the recently published special issue of *Metrologia* devoted to the physics and metrology of electrical charge, which includes papers by Falconer (2004), Bartlett (2004), Unnikrishnan and Gillies (2004), Tu and Luo (2004), Lee *et al* (2004) and Spavieri *et al* (2004).

Acknowledgments

This work was partially supported by the National Key Program of Basic Research Development in China (2003CB716300), the National Natural Science Foundation of China (10121503), and the Foundation for the Authorship of Nationally Excellent Doctoral Dissertations in China (FANEDD: 200220).

References

Abbott L F and Gavela M B 1982 *Nature* **299** 187
Accioly A and Paszko R 2004 *Phys. Rev.* D **69** 107501
Aharonov Y and Bohm D 1959 *Phys. Rev.* **115** 485–91
Aharonov Y and Casher A 1984 *Phys. Rev. Lett.* **53** 319–21
Al'pert Y L, Migulin V V and Ryazin P A 1941 *Zh. Tech. Fiz.* **11** 7–36
Alfvén H 1942 *Nature* **150** 405–6
Alfvén H 1950 *Cosmical Electrodynamics* (London: Oxford University Press)
Alfvén H 1968 *Ann. Geophys.* **24** 341–6
Alfvén H and Carlqvist P 1967 *Solar Phys.* **1** 220–8
Ambjorn J and Wolfram S 1983 *Ann. Phys.* **147** 33–56
Arkani-Hamed N, Dimopoulos S and Dvali G 1998 *Phys. Lett.* B **429** 263–72
Asseo E and Sol H 1987 *Phys. Rep.* **148** 307–436
Barnes A and Scargle J D 1975 *Phys. Rev. Lett.* **35** 1117–20
Barrow J D and Burman R R 1984 *Nature* **307** 14–15
Bartlett D F 2004 *Metrologia* **41** S115–24
Bartlett D F and Lögl S 1988 *Phys. Rev. Lett.* **61** 2285–7
Bartlett D F and Phillips E A 1969 *Bull. Am. Phys. Soc.* **14** 17–18
Bartlett D F, Goldhagen P E and Phillips E A 1970 *Phys. Rev.* D **2** 483–7
Barton G and Dombey N 1984 *Nature* **311** 336–9
Barton G and Dombey N 1985 *Ann. Phys.* **162** 231–72
Bass L and Schrödinger E 1955 *Proc. R. Soc. Lond.* A **232** 1–6

中国科技论文在线 http://www.paper.edu.cn

Bay Z and White J A 1972 *Phys. Rev.* D **5** 796–9
Bicknell G V 1977 *J. Phys. A: Math. Gen.* **10** 407–11
Binney J and Tremaine S 1987 *Galactic Dynamics* (Princeton: Princeton University Press) pp 211–19
Bionta R M *et al* 1987 *Phys. Rev. Lett.* 1494–6
Birge R T 1941a *Rep. Prog. Phys.* **8** 90–134
Birge R T 1941b *Rev. Mod. Phys.* **13** 233–9
Bordag M, Mohideen U and Mostepanenko V M 2001 *Phys. Rep.* **353** 1–205
Boulware D G 1971 *Phys. Rev. Lett.* **27** 55–8
Boulware D G and Deser S 1989 *Phys. Rev. Lett.* **63** 2319–21
Braxmaier C *et al* 2002 *Phys. Rev. Lett.* **88** 010401
Breton V *et al* 1991 *Phys. Rev. Lett.* **66** 572–5
Brown B C 1969 *Nature* **224** 1189
Brown B C *et al* 1973 *Phys. Rev. Lett.* **30** 763–6
Burman R 1972a *J. Phys. A: Gen. Phys.* **5** L128–30
Burman R 1972b *J. Phys. A: Gen. Phys.* **5** L62–3
Burman R 1972c *J. Phys. A: Gen. Phys.* **5** L78–80
Burman R 1973 *J. Phys. A: Math. Nucl. Gen.* **6** 434–44
Burman R R and Byrne J C 1973 *J. Phys. A: Math. Nucl. Gen.* **6** L104–7
Byrne J C 1977 *Astrophys. Space Sci.* **46** 115–32
Byrne J C and Burman R R 1972 *J. Phys. A: Gen. Phys.* **5** L109–11
Byrne J C and Burman R R 1973 *J. Phys. A: Math. Nucl. Gen.* **6** L12–14
Byrne J C and Burman R R 1975 *Nature* **253** 27
Cameron R *et al* 1993 *Phys. Rev.* D **47** 3707–25
Camp J B, Darling T W and Brown R E 1991 *J. Appl. Phys.* **69** 7126–9
Carlqvist P 1969 *Solar Phys.* **7** 377–92
Casimir H B G 1948 *Proc. K. Ned. Akad. Wet.* B **51** 793–6
Casimir H B G and Polder D 1948 *Phys. Rev.* **73** 360–72
Cavendish H 1773 *The Electrical Researches of the Honourable Henry Cavendish* ed J C Maxwell (London: Cambridge University Press 1879) pp 104–13
Chakravorty N N 1985 *Phys. Rev.* D **32** 3334–6
Chen F, Klimchitskaya G L, Mohideen U and Mostepanenko V M 2004 *Phys. Rev.* A **69** 022117
Chernikov M A, Gerber C J, Ott H R and Gerber H J 1992 *Phys. Rev. Lett.* **68** 3383–6
Chernikov M A, Gerber C J, Ott H R and Gerber H J 1992 *Phys. Rev. Lett.* **69** 2999 (erratum)
Chibisov G V 1976 *Usp. Fiz. Nauk* **119** 551–5
Chibisov G V 1976 *Sov. Phys. Usp.* **19** 624–6
Cimmino A *et al* 1989 *Phys. Rev. Lett.* **63** 380–3
Clear J *et al* 1987 *Astron. Astrophys.* **174** 85–94
Cochran G D and Franken P A 1968 *Bull. Am. Phys. Soc.* **13** 1379
Coester F 1951 *Phys. Rev.* **83** 798–800
Crandall R E 1983 *Am. J. Phys.* **51** 698–702
Davies P C W and Toms D J 1985 *Phys. Rev.* D **31** 1363–9
Davis L, Goldhaber A S and Nieto M M 1975 *Phys. Rev. Lett.* **35** 1402–5
De Bernardis P, Masi S, Melchiorri F and Moleti A 1984 *Astrophys. J.* **284** L21–2
De Broglie L 1940 *La Méchanique Ondulatoire du Photon, Une Nouvelle Théorie de Lumière* vol 1 (Paris: Hermann) pp 39–40
Dingus B L *et al* 1988 *Phys. Rev. Lett.* **61** 1906–9
Dirac P A M 1931 *Proc. R. Soc.* A **133** 60
Dirac P A M 1948 *Phys. Rev.* **74** 817–30
Dolgov A D and Zeldovich Y B 1981 *Rev. Mod. Phys.* **53** 1–42
Dombey N 1980 *Nature* **288** 643–4
Dorsey N E 1944 *Trans. Am. Phil. Soc.* **34** 1–110
Eidelman S *et al* 2004 *Phys. Lett.* B **592** 1–1109
Elliott R S 1966 *Electromagnetics* (New York: McGraw-Hill)
Evans M W and Crowell L B 2001 *Classical and Quantum Electrodynamics and the B(3) Field* (Singapore: World Scientific)
Evans M and Vigier J P 1994 *The Enigmatic Photon Volume 1: The field* $\boldsymbol{B}^{(3)}$ (Dordrecht: Kluwer)
Fabian A C and Barcons X 1991 *Rep. Prog. Phys.* **54** 1069–122
Falconer I 2004 *Metrologia* **41** S107–14
Feinberg G 1969 *Science* **166** 879–81

中国科技论文在线 http://www.paper.edu.cn

Feldman G and Matthews P T 1963 *Phys. Rev.* **130** 1633–8
Feynman R P 1949 *Phys. Rev.* **76** 769–89
Fischbach E *et al* 1994 *Phys. Rev. Lett.* **73** 514–7
Florman E F 1955 *J. Res. Natl Bur. Stand.* **54** 335–45
Flowers J L and Petley B W 2001 *Rep. Prog. Phys*. **64** 1191–246
Franken P A and Ampulski G W 1971 *Phys. Rev. Lett.* **26** 115–7
Froome K D 1958 *Proc. Phys. Soc. Lond. Sect.* A **247** 109–22
Froome K D and Essen L 1969 *The Velocity of Light and Radio Waves* (London: Academic)
Fuchs C 1990 *Phys. Rev.* D **42** 2940–2
Fulcher L P 1986 *Phys. Rev.* A **33** 759–61
Fulcher L P and Telljohann M A 1976 *Am. J. Phys.* **44** 366–9
Füllekrug M 2003 *Phys. Rev. Lett.* **93** 043901
Georgi H, Ginsparg P and Glashow S L 1983 *Nature* **306** 765–6
Gerber C J, Chernikov M A and Ott H R 1993 *Rev Sci Instrum.* **64** 793–801
Gillies G T and Ritter R C 1993 *Rev. Sci. Instrum*. **64** 283–309
Gintsburg M A 1963 *Astron. Zh.* **40** 703–9
Gintsburg M A 1964 *Sov. Astron.-AJ* **7** 536–40 (Engl. Transl.)
Ginzburg V L 1970 *The Propagation of Electromagnetic Waves in Plasmas* 2nd edn (Oxford: Pergamon) pp 50–65
Goldhaber A S 1989 *Phys. Rev. Lett.* **62** 482
Goldhaber A S and Nieto M M 1968 *Phys. Rev. Lett.* **21** 567–9
Goldhaber A S and Nieto M M 1971a *Phys. Rev. Lett.* **26** 1390–2
Goldhaber A S and Nieto M M 1971b *Rev. Mod. Phys*. **43** 277–96
Goldhaber A S and Nieto M M 1976 *Sci. Am.* **234** 86–96
Goldhaber A S and Nieto M M 2003 *Phys. Rev. Lett* **91** 149101
Gray R I 1997 *Physics Essays* **10** 342–63
Greiner W and Reinhardt J 1996 *Field Quantization* (New York: Springer) pp 141–70
Hagiwara K *et al* 2002 *Phys. Rev.* D **66** 010001
Haines T J *et al* 1990 *Phys. Rev.* D **41** 692–4
Hawking S W 1979 *General Relativity: An Einstein Centenary Survey* (London: Cambridge University Press)
Heering P 1992 *Am. J. Phys.* **60** 988–94
Hernandez J T 1985 *Phys. Rev.* A **32** 623–4
Hirata K *et al* 1987 *Phys. Rev. Lett.* **58** 1490–3
Hollweg J V 1974 *Phys. Rev. Lett* **32** 961–2
Ignatiev A Y and Joshi G C 1996 *Phys. Rev.* D **53** 984–92
Jackson J D 1975 *Classical Electrodynamics* 2nd edn (New York: Wiley) pp 5–9
Jackson J D and Okun L B 2001 *Rev. Mod. Phys.* **73** 663–80
Johnson J B 1928 *Phys. Rev.* **32** 97–109
Kardar M and Golestanian R 1999 *Rev. Mod. Phys.* **71** 1233–45
Kloor H, Fischbach E, Talmadge C and Greene G L 1994 *Phys. Rev.* D **49** 2098–113
Kobzarev I Y and Okun L B 1968 *Usp. Fiz. Nauk* **95** 131–7
Kobzarev I Y and Okun L B 1968 *Sov. Phys. Usp* **11** 338–41 (Engl. Transl.)
Kohler C 2002 *Class. Quantum Grav.* **19** 3323–31
Kostelecký V A and Samuel S 1991 *Phys. Rev. Lett* **66** 1811–14
Krause D E, Kloor H T and Fischbach E 1994 *Phys. Rev.* D **49** 6892–909
Kroll N M 1971 *Phys. Rev. Lett.* **26** 1395–8
Kronberg P P 1994 *Rep. Prog. Phys.* **57** 325–82
Kronberg P P 2002 *Physics Today* **55** 40–6
Lakes R 1998 *Phys. Rev. Lett.* **80** 1826–9
Lamoreaux S K 1997 *Phys. Rev. Lett.* **78** 5–8
Langel R A and Estes R H 1985 *J. Geophys. Res.* **90** 2495–509
Lee E R, Halyo V, Lee I T and Perl M L 2004 *Metrologia* **41** S147–58
Lehnert B 1954 *Phys. Rev.* **94** 815–24
Lehnert B 2000 *J. New Energy* **5** 81–7
Lehnert B and Roy S 1998 *Extended Electromagnetic Theory: Space-Charge in Vacuo and the Rest Mass of the Photon* (Singapore: World Scientific)
Lipa J A *et al* 2003 *Phys. Rev. Lett.* **90** 060403
Lovell B, Whipple F L and Solomon L H 1964 *Nature* **202** 377
Lowenthal D D 1973 *Phys. Rev.* D **8** 2349–52

中国科技论文在线 http://www.paper.edu.cn

Luckey D and Weil J W 1952 *Phys. Rev.* **85** 1060
Lundquist S 1949 *Phys. Rev.* **76** 1805–9
Luo J, Shao C C, Liu Z Z and Hu Z K 2000 *Phys. Lett.* A **270** 288–92
Luo J, Tu L C, Hu Z K and Luan E J 2003 *Phys. Rev. Lett.* **90** 081801
Luo J, Tu L C, Hu Z K and Luan E J 2003 *Phys. Rev. Lett.* **91** 149102
Manchester R N 1974 *Astrophys. J.* **188** 637–44
Mandelstam L I and Papalexi N D 1944 *Usp. Fiz. Nauk.* **26** 144–68
Mansouri R M and Sexl R U 1977 *Gen. Relativ. Gravit.* **8** 497–513
Masood S S 1991 *Phys. Rev.* D **44** 3943–8
Maxwell J C 1873 *A Treatise on Electricity and Magnetism* 3rd edn (New York: Dover) pp 80–6
Mendonça J T, Martins A M and Guerreiro A 2000 *Phys. Rev.* E **62** 2989–91
Michaelson H B 1977 *J. Appl. Phys.* **48** 4729–33
Milton K A 2001 *The Casimir Effect* (Singapore: World Scientific)
Mohapatra R N 1987 *Phys. Rev. Lett.* **59** 1510–12
Mostepanenko V M and Trunov N N 1997 *The Casimir Effect and its Applications* (Oxford: Clarendon)
Müller H *et al* 2003a *Phys. Rev.* D **67** 056006
Müller H *et al* 2003b *Phys. Rev. Lett.* **91** 020401
Mulligan J F 1952 *Am. J. Phys.* **20** 165–72
Mulligan J F 1976 *Am. J. Phys.* **44** 960–9
Mulligan J F and McDonald D F 1957 *Am. J. Phys.* **25** 180–92
Nieuwenhuizen P 1973 *Phys. Rev.* D **7** 2300–8
Norman T and Setterfield B 1987 *The Atomic Constants Light and Time* (Menlo Park, CA: SRI International)
Nussinov S 1987 *Phys. Rev. Lett.* **59** 2401–4
Nyqyist H 1928 *Phys. Rev.* **32** 110–13
Park D and Williams E R 1971 *Phys. Rev. Lett.* **26** 1393–4
Patel V L 1965 *Phys. Lett* **14** 105–6
Patel V L and Cahill L J 1964 *Phys. Rev. Lett.* **12** 213–14
Plimpton S J and Lawton W E 1936 *Phys. Rev.* **50** 1066–71
Primack J R and Sher M A 1980 *Nature* **288** 680–1
Proca A 1930a *Compt. Rend.* **190** 1377–9
Proca A 1930b *Compt. Rend.* **191** 26–9
Proca A 1930c *J. Phys. Radium Ser. VII* **1** 235–48
Proca A 1931 *Compt. Rend.* **193** 832–4
Proca A 1936a *Compt. Rend.* **202** 1366–8
Proca A 1936b *Compt. Rend.* **202** 1490–2
Proca A 1936c *Compt. Rend.* **203** 709–11
Proca A 1936d *J. Phys. Radium Ser. VII* **7** 347–53
Proca A 1937 *J. Phys. Radium Ser. VII* **8** 23–8
Proca A 1938 *J. Physique Ser. VII* **9** 61–6
Prokopec T, Törnkvist O and Woodard R 2002 *Phys. Rev. Lett.* **89** 101301
Rand R J and Kulkarni S R 1989 *Astrophys. J.* **343** 760–72
Robertson H P 1949 *Rev. Mod. Phys.* **21** 378–82
Ryan J J, Accetta F and Austin R H 1985 *Phys. Rev.* D **32** 802–5
Ryutov D D 1997 *Plasma Phys. Control. Fusion* **39** A73–82
Saathoff G *et al* 2003 *Phys. Rev. Lett.* **91** 190403
Scargle J D 1969 *Astrophys. J.* **156** 401–26
Schaefer B E 1999 *Phys. Rev. Lett.* **82** 4964–6
Schrödinger E 1943a *Proc. R. Ir. Acad.* A **49** 135–48
Schrödinger E 1943b *Proc. R. Ir. Acad.* A **49** 43–58
Singleton D 1996 *Int. J. Theor. Phys.* **35** 2419–26
Spavieri G, Gillies G T and Rodriguez M 2004 *Metrologia* **41** S159–70
Staelin D H and Reifenstein III G C 1968 *Science* **162** 1481–3
Strocchi F 1967 *Phys. Rev.* **162** 1429–38
Stueckelberg E C G 1941 *Helv. Phys. Acta* **14** 51–80
Stueckelberg E C G 1957 *Helv. Phys. Acta* **30** 209–15
Sugiura M 1961 *Phys. Rev. Lett.* **6** 255–7
Suzuki M 1988 *Phys. Rev.* D **38** 1544–50
Taylor B N, Parker W H and Langenberg D N 1969 *Rev. Mod. Phys.* **41** 375–496

中国科技论文在线 http://www.paper.edu.cn

Thompson D J, Fichtel C E, Kniffen D A and Ögenman H B 1975 *Astrophys. J.* **200** L79–82
Tonomura A *et al* 1986 *Phys. Rev. Lett.* **56** 792–5
Tu L C and Luo J 2004 *Metrologia* **41** S136–46
Unnikrishnan C S and Gillies G T 2004 *Metrologia* **41** S125–35
Vigier J P 1990 *IEEE Trans. Plasma Sci.* **18** 64–72
Vigier J P 1992 *Present Experimental Status of the Einstein–de Broglie Theory of Light* (Tokyo: Proc. ISQM Workshop on Quantum Mechanics)
Vigier J P 1997 *Phys. Lett.* A **234** 75–85
Warner B and Nather R E 1969 *Nature* **222** 157–8
Wilkie T 1983 *New Sci.* **100** 258–63
Williams E and Park D 1971 *Phys. Rev. Lett.* **26** 1651–2
Williams E R, Faller J E and Hill H A 1970 *Bull. Am. Phys. Soc.* **15** 586–7
Williams E R, Faller J E and Hill H A 1971 *Phys. Rev. Lett.* **26** 721–4
Wolf P *et al* 2003 *Phys. Rev. Lett.* **90** 060402
Yamaguchi Y 1959 *Prog. Theor. Phys. (Japan)* **11** (Suppl.) 1–36
Young B C, Cruz F C, Itano W M and Bergquist J C 1999 *Phys. Rev. Lett.* **82** 3799–802
Zhang Y Z 1998 *Speical Relativity and its Experimental Foundations* (Singapore: World Scientific) pp 245–67
Zwiebel E 1991 *Nature* **352** 755–6
Zygan H 1970a *Phys. Lett.* A **33** 293–4
Zygan H 1970b *Phys. Lett.* A **32** 90–1